Effects of ship emissions on air quality in the Baltic Sea region simulated with three different chemistry transport models

Matthias Karl[1], Jan Eiof Jonson[2], Andreas Uppstu[3], Armin Aulinger[1], Marja Prank[3,4],
Jukka-Pekka Jalkanen[3], Lasse Johansson[3], Markus Quante[1], and Volker Matthias[1]

[1]Institute of Coastal Research, Helmholtz-Zentrum Geesthacht, 21502 Geesthacht, Germany.
[2]Norwegian Meteorological Institute, Oslo, Norway.
[3]Atmospheric Composition Research, Finnish Meteorological Institute, P.O. Box 503 FI-00101 Helsinki, Finland.
[4]now at: Cornell University, Ithaka, NY, U.S.A..

Correspondence: M. Karl (matthias.karl@hzg.de)

Abstract. The Baltic Sea is highly frequented shipping area with busy shipping lanes close to densely populated regions. Exhaust emissions from ship traffic into the atmosphere are not only enhancing air pollution, they also affect the Baltic Sea environment through acidification and eutrophication of marine waters and surrounding terrestrial ecosystems. As part of the European BONUS project SHEBA (Sustainable Shipping and Environment of the Baltic Sea Region), the transport, chemical

5 transformation and fate of atmospheric pollutants in the Baltic Sea region was simulated with three regional chemistry transport models (CTM) systems, CMAQ, EMEP/MSC-W and SILAM with grid resolutions between 4 km and 11 km. The main goal was to quantify the effect that shipping emissions have on the regional air quality in the Baltic Sea region when the same shipping emissions dataset but different CTMs in their typical setups are used. The performance of these models and the shipping contribution to the results of the individual models was evaluated for sulphur dioxide (SO_2), nitrogen dioxide (NO_2)

10 and ozone (O_3) and particulate matter ($PM_{2.5}$). Model results from the three CTMs were compared to observations from rural and urban background stations of the AirBase monitoring network in the coastal areas of the Baltic Sea region. The performance of the three CTM systems to predict pollutant concentrations is similar. However, observed $PM_{2.5}$ in summer was underestimated strongly by CMAQ and to some extent by EMEP/MSC-W. The spatial average of annual mean O_3 in the EMEP/MSC-W simulation is 15–25 % higher compared to the other two simulations, which is mainly the consequence of

15 using a different set of boundary conditions for the European model domain. There are significant differences in the calculated ship contributions to the levels of air pollutants among the three models. SILAM predicted a much weaker ozone depletion through NO emissions in the proximity of the main shipping routes than the other two models. In the entire Baltic Sea region the average contribution of ships to $PM_{2.5}$ levels is in the range of 4.3–6.5 % for the three CTMs. Differences in ship-related $PM_{2.5}$ between the models are mainly attributed to differences in the schemes for inorganic aerosol formation. Inspection

20 of the ship-related elemental carbon (EC) revealed that assumptions about the vertical ship emission profile can affect the dispersion and abundance of ship-related pollutants in the near-ground atmosphere. The models are in agreement regarding the ship-related deposition of oxidised nitrogen, reporting a ship contribution in the range of 21–23 ktN y^{-1} as atmospheric input to the Baltic Sea. Results from the present study show the sensitivity of the ship contribution to combined uncertainties of boundary conditions, meteorological data and aerosol formation and deposition schemes. This is an important step towards

Atmospheric
Chemistry
and Physics
Discussions

a more reliable evaluation of policy options regarding emission regulations for ship traffic and the planned introduction of a nitrogen emission control area (NECA) in the Baltic Sea and the North Sea in 2021.

1 Introduction

International shipping is important for the economic exchange in Europe: almost 90 % of the European Union (EU) import and export freight trade is seaborne. Compared to other modes of transport such as trucks and air freight, shipping is far more energy efficient per ton of cargo. The Baltic Sea is one of the most densely trafficked sea regions in the world. Roughly 407,500 ship crossings in the Baltic Sea were recorded in 2012 (HELCOM, 2014), including passenger, cargo, tanker and other ship types. Maritime transport of goods between main EU ports and ports located in the Baltic Sea has a share of 22 % (in 2016) of the total shipping tonnages within European seas (EUROSTAT, 2018).

Ship traffic is associated with exhaust emissions of a wide range of air pollutants, among them nitrogen oxides ($NO_X = NO + NO_2$), black carbon (BC), sulphur dioxide (SO_2), non-methane volatile organic compounds (NMVOC) and particulate matter, as well as greenhouse gases (mainly carbon dioxide, CO_2). Primary and secondary particulate matter from ship exhaust has been associated with adverse health effects (e.g. Corbett et al., 2007). The emitted amounts and size spectrum of particulate matter depends on the type of fuel and its sulphur content and the ship engine type (e.g. Fridell et al., 2008; Moldanová et al., 2009). For regulatory purposes, particulate matter is divided into the size fractions PM_{10} and $PM_{2.5}$ according to aerodynamic diameter, where PM_{10} covers all particles with diameter less than 10 μm and $PM_{2.5}$ those with diameter less than 2.5 μm. A global model study by Sofiev et al. (2018b) demonstrated the health benefits from reducing the ship-related fine particulate matter by low-sulphur ship fuels in densely populated, major-trading nations.

Emissions from ships are transported in the atmosphere over several hundreds of kilometres (Endresen et al., 2003). The atmospheric transformation of primary emitted gases from shipping is especially relevant for the formation of O_3 and the deposition of sulphur and nitrogen compounds distant from the ship lanes (Eyring et al., 2010). Exhaust emissions from ship traffic in the Baltic Sea has the potential to degrade air quality in the coastal areas (Jonson et al., 2015) and to significantly affect the Baltic Sea environment through acidification and eutrophication of marine waters and surrounding terrestrial ecosystems (HELCOM, 2009; Bartnicki et al., 2011; Hunter et al., 2011; Raudsepp et al., 2013; Neumann et al., 2018a, b, c). Acidification is a major challenge in the Baltic Sea region today where the critical load (CL) for acidification is exceeded especially in the southern part (Tsyro et al., 2018). The CL for acid deposition is the value that must not be exceeded in order to maintain the soil's capacity to neutralise the excess acid. Between 2000 and 2016, the percentage of ecosystem areas in Europe where CL (acidification) was exceeded decreased from 16 % to 6 % (Tsyro et al., 2018), partially as a result of stricter sulphur regulations for ships. Despite the considerable improvement concerning critical loads with respect to acidification, there are still regions in the Baltic Sea catchment, for which further reductions in acidification are desirable (Hettelingh et al., 2017). Atmospheric deposition of nitrogen compounds play a role in the eutrophication of the coastal marine environment (e.g., Paerl, 1995) and threaten biodiversity in forests, semi-natural vegetation, and freshwater catchments through excessive nitrogen input (Cofala

et al., 2007). Even though exceedances of CL for eutrophication has decreased over the past decades, critical loads are still exceeded in about 65 % of the European ecosystems (Tsyro et al., 2018).

Air pollution from ships is increasingly controlled worldwide by the International Maritime Organization (IMO) through the Marine Pollution Convention (MARPOL) Annex VI - Regulations for the Prevention of Air Pollution from Ships (IMO, 2008).

5 The Baltic Sea has been a sulphur emission control area (SECA) since May 2006, with stepwise reductions of the sulphur content in ship fuels; from 2015 onwards the sulphur content of any fuel oil used on-board ships within the Baltic Sea has to be 0.1 % or less (van Aardenne et al., 2013). The MARPOL regulations on emissions of NO_X (TIER) are defined as function of year of installation and vessel speed. The TIER I standard was introduced in 2000 and is up to 10 % stricter than for ships built before 2000. TIER II was implemented in 2011 applying 15 % stricter standards than TIER I. The effect of regulations of

10 nitrogen emissions have been small until now, as these are only enforced for the new built ships. A nitrogen emission control area (NECA) for the Baltic Sea, North Sea and English Channel will become effective in 2021, in which new built ships have to comply with TIER III, approximately 75 % stricter than TIER II. The consequences of establishing the NECA on the future air quality in the Baltic Sea region are investigated in the companion paper by Karl et al. (2018).

The transport, chemical transformation and fate of atmospheric pollutants in the Baltic Sea region can be simulated with 3-D

15 chemistry transport model (CTM) systems. Previous air quality model studies related to shipping in the North Sea and Baltic Sea (Matthias et al., 2010; Hongisto, 2014; Jonson et al., 2015, 2018b; Matthias et al., 2016;Antturi et al., 2016; Claremar et al., 2017) used CTM systems to investigate the effect of implementation of MARPOL regulations on sulphur emissions by ships, the effect of establishing the NECA and other ship emission control scenarios. The studies quantified the contributions from shipping to the total air concentrations, deposition of nitrogen and sulphur, as well as air quality and health indicators.

20 Jonson et al. (2018b) studied the effects of shipping on the global scale, including the effects of shipping in the Baltic Sea and the North Sea, compared to total anthropogenic emissions in a global CTM with 0.5×0.5 degrees resolution. They found that a significant fraction, ranging from 5 % to more than 10 %, of the $PM_{2.5}$ and the depositions of nitrogen of anthropogenic origin in bordering countries can be attributed to ship emissions in the two sea areas. For the deposition of sulphur, ship emission contributions are markedly lower as a result of the implementation of a stricter SECA (from 2015 onwards). For ground level

25 O_3 contributions were found to vary depending on country and the choice of ozone metric ranging from negative contributions for annual average ozone to more than 10 % of the summertime phytotoxic ozone dose (POD1) for forests in some countries in the Baltic Sea region.

On the regional scale, Jonson et al. (2015) using the EMEP/MSC-W model (Simpson et al., 2012) with a horizontal resolution of $14 \times 14 \, km^2$ assessed the effect of reduced sulphur content (2015 value of 0.1 %) and regulation of NECAs on the air

30 quality, deposition of nitrogen and related impacts on human health in the Baltic and North seas. Matthias et al. (2016) used the Community Multiscale Air Quality (CMAQ) model v4.7.1 (Byun and Schere, 2006) with a horizontal resolution of $24 \times 24 \, km^2$ to investigate the effects of different future developments of shipping emissions in the North Sea area on air quality in the North Sea region. Antturi et al. (2016) used the SILAM (Sofiev et al., 2015) CTM system with spatial resolution of ca. $8 \times 8 \, km^2$ in a cost-benefit analysis of the sulphur reduction policy in the Baltic Sea, but did not investigate the effects of shipping emissions

35 on ozone concentration or nitrogen deposition. The study by Claremar et al. (2017) used the EMEP/MSC-W model with a much

coarser resolution ($50 \times 50\,km^2$) and gridded shipping emissions from the ENTEC inventory (Jonson et al., 2009) for 2011 and from TNO-MACC-III (Gauss et al, 2015) for 2013. They find highest contribution of international shipping in the Baltic Sea and North Sea near large harbour cities and along the main shipping lanes; with contributions to ambient levels of nitrogen dioxide (NO_2), SO_2, PM_{10}, and $PM_{2.5}$ of about 80 %, 80 %, 13 %, and 20 %, respectively (Claremar et al., 2017).

5   The use of relatively coarse model grids (coarser than 10-km resolution) in some of the previous CTM simulations raises concerns about non-linear chemical effects, particularly for O_3, since a high source strength from shipping in the proximity to large land-based emissions (inside the same grid cell of the model) often results in very high levels of NO_X and excessive ozone titration (Jonson et al., 2009). Moreover, shipping releases large amounts of NO_X from a point source within the relatively clean maritime atmosphere. In regional CTMs, these NO_X emissions are diluted into large grid volumes, which can lead to

10   a systematic overestimation of the ozone production and artificially increases the lifetime of NO_X (Von Glasow et al., 2003; Song et al., 2003; Vinken et al., 2011).

In the Baltic Sea area, movements of ships are gathered in the regional HELCOM (Baltic Marine Environment Protection Commission - Helsinki Commission) Automatic Identification System (AIS) network and database (http://maps.helcom.fi/website/AISexplorer/). Not all previous air quality studies in the Baltic Sea region used AIS ship position data, some use long

15   averaging intervals for shipping emissions. For the North Sea region, Matthias et al. (2016) designed emission control scenarios based on a detailed emission inventory built upon AIS ship positions and a detailed ship characteristics database (Aulinger et al., 2016). The studies by Antturi et al. (2016) and Jonson et al. (2015) deployed the Ship Traffic Emission Assessment Model (STEAM; Jalkanen et al., 2009, 2012) which combines the AIS-based information with the detailed technical knowledge of the individual ships.

20   Despite previous model based work on the effects of shipping on air quality and human health in the Baltic Sea region, there is a need for more localised studies building on a much higher level of details, i.e. concerning shipping activity, for the quantification of regional ship-related air pollution. Knowledge on air quality impacts of shipping with a finer spatial resolution than in previous model studies is required for the identification of best suited sustainable development options for the shipping sector, especially if a varying suite of competing environmental and economic drivers is to be considered in different sub-

25   regions.

With the goal to support EU policies on environmental and economic aspect of the shipping sector the BONUS project SHEBA (Sustainable Shipping and Environment of the Baltic Sea Region; http://www.sheba-project.eu) was established in 2015. The overarching aim of BONUS SHEBA was an integrated and in-depth analysis of the ecological, economic and social impacts of shipping in the Baltic Sea. The project brought together experts from many different fields (and 11 partner

30   institutions) in order get a complete picture of the environment impact. Within SHEBA the fate of pollutants into water and air emitted by sea going ships and ships at berth was assessed, both for the present-day situation as well as for several developed scenarios of shipping in the intermediate future. The task was building mainly on a suite of consecutive models following pollutants on the path from emission via dispersion to impacts in target regions.

As part of the SHEBA project, the transport, chemical transformation and fate of atmospheric pollutants in the Baltic Sea

35   region was simulated with three different regional CTM systems (CMAQ, EMEP/MSC-W and SILAM) to investigate the effect

of ship emissions on the regional air quality in the Baltic Sea region. The chosen CTM systems are well established in Europe and have been extensively tested in several multi-model assessment studies (Solazzo et al., 2012a, 2012b, 2013, 2017; Vautard et al., 2012; Colette et al., 2011, 2012; Langner et al., 2012; Vivanco et al., 2018). Prank et al. (2016) evaluated the skill of air quality models including SILAM, EMEP, and CMAQ to reproduce the particulate matter concentration and composition on

5 European scale. EMEP/MSC-W (from MET Norway) and SILAM (from FMI) are part of the operational Copernicus Atmosphere Monitoring Service (CAMS; http://www.regional.atmosphere.copernicus.eu/) regional air quality ensemble for Europe. All three models have been used previously in the North Sea and Baltic Sea region for estimating the effect of shipping (Jonson et al., 2015; Antturi et al., 2016; Matthias et al., 2010, 2016). The model setup with CMAQ used in Matthias et al. (2016) has been evaluated for the larger North Sea region (Aulinger et al., 2016).

10 The EMEP/MSC-W model (at MET Norway) is also included with the same model configuration in the Baltic Sea region Interreg project EnviSuM (Environmental Impact of Low Emission Shipping: Measurements and Modelling Strategies). The main focus of the EnviSuM project is on sulphur emissions from shipping. EnviSuM investigates the effects of the implementation of the stricter SECA from 2015 onwards, combining measurements and modelling. This includes measurements of emissions from ships applying different technologies as for instance low sulphur oil, scrubber technology, and liquefied natural

15 gas (LNG). The improved emission estimates are used in chemical tracer models calculating the effects on air pollution and depositions and subsequent effects on human health and ecosystems.

This study takes a multi-model approach using three CTM systems to assess the uncertainties connected with the atmospheric transport and transformation of air pollutants. The comparison of air concentration of regulatory pollutants between the models is the primary focus of this study. However, the annual average nitrogen deposition fields were also compared due

20 to the relevance of atmospheric nitrogen deposition for the eutrophication of the coastal marine environment. In the western Baltic Sea, with its specific coastal features such as boddens and lagoons, the grid resolution of atmospheric CTMs has been found to strongly impact on the modelled nitrogen deposition (Neumann et al., 2018a). Model results from the three CTMs for NO_X, O_3, SO_2 and $PM_{2.5}$ are compared to observations from rural and urban background stations in the coastal areas of the Baltic Sea region. Statistical performance analysis of the comparison of modelled against observation data was carried out for

25 all CTM systems and the performance of the models was inter-compared based on several statistical indicators. Specifically, we want to evaluate the contribution of shipping emissions to modelled surface concentrations of important air pollutants. The significance of ship contribution to ambient NO_2 observations at coastal monitoring stations is evaluated for the different models. The use of three CTM systems, together with comparison to ground-based observations, provides a comprehensive view on the current air quality situation of the Baltic Sea region and how it is affected by emissions from shipping. The combination

30 of three CTM also provides a more robust estimate of the ship-related contribution to ambient atmospheric concentrations.

2 Description of the CTM systems and setup of the model comparison

The setup of the three CTM systems for this study with respect to drivers for meteorology, boundary conditions and emissions was specific for each model system. The models were set up in a way as they are typically used in air quality studies in

European regions. However, the applied CTMs use a much higher spatial and temporal resolution as previous modelling of the air quality in the Baltic Sea region. Shipping activities are considered with a high degree of detail in the simulations; using AIS position data and up-to-date load dependent emission factors for all important air pollutants. The dynamic ship emission inventory STEAM was applied in all CTMs. STEAM takes into account the emission control areas and regulations, emission

5   abatement equipment on-board the ships as well as fuel sulphur content modelling separately for main and auxiliary engines (Johansson et al., 2017; Jalkanen et al., 2012). All three regional air quality models implement state-of-the-art formulations of atmospheric transport, atmospheric chemistry and aerosol formation, updated compared to the model versions used in the previous studies. Partly the same or similar drivers for anthropogenic emissions were used in the CTMs. Ship exhaust emission from the North Sea are handled in the same manner as the Baltic Sea emissions since they affect the western part of the

10   Baltic Sea region. By this procedure it is ensured, that all interactions of shipping emissions with pollutants in the regional background and from land-based emission sources are correctly considered. With all models a reference run for the current air quality situation was performed including all emissions ("base") and one run without the emissions from shipping ("noship"). The difference between the run with all emissions and the run without shipping emissions is used to determine the contribution of ships to the ambient pollutant concentration.

15   ## 2.1   Description of the models

2.1.1   CMAQ model

The CMAQ model v5.0.1 (Byun and Schere, 2006; Appel et al., 2013; 2017) computes the air concentration and deposition fluxes of atmospheric gases and aerosols as a consequence of emission, transport and chemical transformation. The atmospheric chemistry is treated by the modified Carbon Bond V mechanism cb05tucl with updated toluene chemistry and chlorine radical

20   chemistry (Yarwood et al., 2005; Whitten et al., 2010; Sarwar et al., 2012). The aerosol scheme AERO5 is used for the formation of secondary inorganic aerosol (SIA). The gas phase/aerosol equilibrium partitioning of sulphuric acid (H_2SO_4), nitric acid (HNO_3), hydrochloric acid (HCl) and ammonia (NH_3) is solved with the ISORROPIA v1.7 mechanism (Fountoukis et al., 2007; Nenes et al., 1999). The formation of secondary organic aerosol (SOA) from isoprene, monoterpenes, sesquiterpenes, benzene, toluene, xylene, and alkanes (Carlton et al., 2010; Pye and Pouliot, 2012) is included.

25   The dry deposition parameterization is presented in Binkowski and Shankar (1995) and Binkowski and Roselle (2003). Wet deposition of gases and particles is computed by the resolved cloud model of CMAQ which estimates how much certain vertical model layers contributed to the precipitation (Foley et al., 2010). Sea salt emissions were calculated inline by the parameterization of Gong (2003) (as described in Kelly et al., 2010. Sea salt surf zone emissions were deactivated because of considerable overestimations in some coastal regions (Neumann et al., 2016). Biogenic emissions (NMVOC from vegetation

30   and soil NO) were calculated off-line with the biogenic Emission Inventory System BEIS v3.4 (Schwede et al., 2005; Vukovich and Pierce, 2002). Emissions of wind-blown dust were not considered.

The Meteorology-Chemistry Interface Processor (MCIP; Otte and Pleim, 2010) processes meteorological model output into the input format required for CMAQ. The vertical dimension of the model extends up to 100 hPa in a sigma hybrid pressure

Atmospheric
Chemistry
and Physics
Discussions

coordinate system with 30 layers. Twenty of these layers are below approximately 2 km; the lowest layer extends to ca. 36 m above ground. A spin-up period of one month (December 2011) was used for the initialization of the model runs, sufficiently long to prevent that initial conditions have an effect on the simulated atmospheric concentrations of the investigated period (year 2012).

2.1.2 SILAM model

The SILAM (System for Integrated modeLling of Atmospheric coMposition) model v5.5 (Sofiev et al., 2015; http://silam.fmi.fi/) was used as second CTM in this study. The gas phase chemistry was simulated with the Carbon Bond (CB) mechanism CBM-IV, with reaction rates updated according to the recommendations of the International Union of Pure and Applied Chemistry (IUPAC, http://iupac.pole-ether.fr) and the NASA Jet Propulsion Laboratory (JPL; http://jpldataeval.jpl.nasa.gov) and the terpenes oxidation added from CB05 reaction list (Yarwood et al., 2005). The sulphur chemistry and secondary inorganic aerosol formation is computed with an updated version of the DMAT scheme (Sofiev, 2000) and secondary organic aerosol formation with the Volatility Basis Set (VBS, Donahue et al., 2011), the volatility distribution of anthropogenic organic carbon taken from Shrivastava et al. (2011). Organic aerosol in SILAM was evaluated in a recent study by Prank et al. (2018).

The dry deposition scheme is described in Kouznetsov and Sofiev (2012) and the wet deposition in Kouznetsov and Sofiev (2013). Natural emissions included in the simulations are sea-salt emissions as in Sofiev et al. (2011), biogenic NMVOC emissions as in Poupkou et al. (2010); wild-land fire emissions as in Soares et al. (2015) and wind-blown desert dust.

SILAM includes a meteorological pre-processor for diagnosing the basic features of the boundary layer and the free troposphere from the meteorological fields provided by various meteorological models (Sofiev et al., 2010). In total 10 vertical layers, extending up to 2000 m above the surface, are included. The lowest layer extends to 20 m above the surface. No spin-up period was applied.

2.1.3 EMEP/MSC-W model

The third CTM used in this study is the EMEP/MSC-W chemical transport model, version rv4.8. This model, available as open source (https://github.com/metno/emep-ctm), has been described in detail in Simpson et al. (2012), with various updates, see Simpson et al. (2016) and references within. Chemistry scheme of the gas-phase in the model is EmChem09, having 72 chemical compounds including 10 "surrogate" VOCs, out of which isoprene represents BVOCs, and 137 reactions. This scheme is an update of previous chemical schemes (e.g. Simpson, 1992; Andersson-Sköld and Simpson, 1999). The EMEP scheme involves relatively more details on peroxy radical (RO_2) chemistry than e.g. Carbon Bond (CB) schemes. SOA is calculated using a VBS scheme, which tracks the semi volatile products of VOC oxidation, and dynamically partitions these between the gas and aerosol phases (e.g. Robinson et al., 2007). A number of schemes were tested in Bergström et al. (2012), but here the standard "NPAS" scheme as described in Simpson et al. (2012) is used.

For Europe the model is regularly evaluated against measurements in the EMEP annual reports, see www.emep.int. In addition the EMEP model has been included in model inter-comparisons and model validations in a number of peer reviewed publications (Jonson et al., 2006, 2010, 2018a; Simpson et al., 2006a, 2006b; Colette et al., 2011, 2012; Angelbratt et al., 2011;

Dore et al., 2015; Stjern et al., 2016). Biogenic emissions (NMVOC, soil NO), emissions of dimethyl sulphide (DMS) from oceans, sea-salt, dust, road dust, emissions from aviation on cruising altitude, lightning, volcanic emissions and emissions from forest fires are included as separate databases or calculated within the model (EMEP, 2015).

EMEP is driven by the meteorological data of the European Centre for Medium-Range Weather Forecasts (ECMWF) based on the Cy40r1 version. An important addition to the forecast ensemble in cycle Cy40r1 has been the introduction of ocean-atmosphere coupling from day 0, instead of from day 10 as in the previous cycles. Vertically, the meteorological fields from ECMWF are interpolated onto 20 EMEP sigma levels, between the surface and 100 hPa. Initial and boundary concentrations are based on long-term observations and some model data. No spin-up period was applied.

2.2 Setup of the CTM systems

The CTMs were offline coupled with different meteorological models (COSMO-CLM, ECMWF-IFS, and WRF). CMAQ and SILAM were operated with high horizontal resolution (4 km) on the inner nest representing the Baltic Sea region starting from simulations of a coarser European domain. EMEP MSC-W was operated on 0.1 degree resolution for the whole of Europe. Ship emissions from the STEAM model (Jalkanen et al., 2009; Jalkanen et al., 2012 Johansson et al., 2013), which use ship position data of the HELCOM AIS network, were gridded to the respective model's grid resolution. Land-based emissions were from SMOKE-EU (Bieser et al., 2011a) or ECLIPSE (Amann et al., 2012; Amann et al., 2013) databases; annual totals were comparable.

2.2.1 Model domains and nesting

The spatial extent for the intercomparison study covers the Baltic Sea region, spanning from latitude 53.50°N (south) to 66.00°N (north) and longitude 9.00°E (west) to 31.00°E (east). Parts of the Kattegat and a small part of the Norwegian Sea is covered by the extent, but not considered in the comparison. The extent of the geographic domain is displayed in Fig. 1. Nested simulations were done with CMAQ and SILAM models, using the output of the finer resolved inner nest whereas the simulation with the EMEP/MSC-W model covered the European domain. The SILAM model was operated on rotated grids centred on the respective domain. The horizontal grid resolution of the output was 4 km for CMAQ, 0.04 degrees (~4 km) for SILAM and 0.1 degrees (~11 km) for EMEP/MSC-W. Note that the grid distance in x-direction becomes smaller with increasing latitude (for instance, 0.1° in longitude corresponds to 6.2 km at 56°N). Different drivers were used for meteorological simulations coupled offline to the CTM simulations. Anthropogenic emissions from the continent and the shipping emissions in the North and Baltic seas were identical (CMAQ and SILAM) or similar in spatial distribution and magnitude (EMEP/MSC-W). The EMEP/MSC-W model used monthly averaged gridded ship emissions, while the other two models used hourly emissions. Daily or hourly emissions reflect ship traffic pattern changes due to meteorological conditions or due to sea ice. Using a coarser time resolution for shipping thus mainly neglects the influence of weather and ice on ship operations (Jonson et al., 2015). Table 1 gives an overview of the model setups of the three CTM systems for use in the intercomparison study.

Nested simulations with CMAQ were performed with a coarse outer domain for entire Europe with grid cell size of $64 \times 64 \, km^2$, an intermediate domain with $16 \times 16 \, km^2$ for Northern Europe and an inner domain with a horizontal resolution of $4 \times 4 \, km^2$ for the entire Baltic Sea. Model results for the intercomparison were taken from the inner domain for the coastal regions and from the intermediate domain for parts of Sweden, Finland and the Baltic states. For details on the high-

5 resolution output from CMAQ and an evaluation of the model setup with a limited number of regional background stations, it is referred to Karl et al. (2018).

For the SILAM model, the grid cell size was roughly $70 \times 70 \, km^2$ for the outer domain, roughly $18 \times 18 \, km^2$ for the central domain, and roughly $4 \times 4 \, km^2$ for the inner domain. The simulation time steps were 20 min, 10 min, and 4 min, respectively. Model results for the intercomparison were mostly from the inner domain, with parts of Finland and eastern Europe from the

10 central domain. SILAM took part in AQMEII 1 and 3 intercomparisons showing comparable performance with other European state-of-the-art air quality models (Solazzo et al., 2012a, 2012b, 2013, 2017; Vivanco et al., 2018; Marécal et al., 2015). The EMEP/MSC-W model was run with a 0.1×0.1 degrees resolution for whole Europe. A comprehensive description, including model evaluations, of the model results with the 0.1×0.1 degrees application of the EMEP model for 2013 can be found in Tsyro et al. (2015).

15 **2.2.2 Meteorology**

The SILAM model is run with meteorological input from a simulation with the Weather Research and Forecast (WRF) model v3.7.1 using original resolutions of 4.0 km, 16.0 km, and 64.0 km, for inner, central and outer domains, respectively. In general, linear interpolation was applied for the simulation, but conservation of mass was used where applicable. High-resolution meteorological fields for CMAQ were obtained from the COSMO-CLM (Rockel et al., 2008) model v5.0. More

20 details on the meteorological forcing data and the evaluation of precipitation can be found in Karl et al. (2018). The meteorological fields were converted to the extension, resolution and projection of the CMAQ nested grids, using an in-house modified version of MCIP. EMEP/MSC-W was driven by meteorological data from the Integrated Forecasting System (IFS) of the ECMWF, version IFS38r2, with t1279 resolution (about 0.16 degrees resolution) interpolated to 0.1×0.1 degrees.

The use of different meteorological datasets introduces additional variability which is on one hand wanted to achieve a wider

25 range of possible results for estimating the effect of shipping on air quality but on the other hand complicates the interpretation of differences between the models.

2.2.3 Boundary conditions

The initial conditions (ICONs) for the simulation and the lateral boundary conditions (BCONs) for the outer European domain are taken from FMI APTA global reanalysis (Sofiev et al., 2018a)). The global boundary conditions results have been inter-

30 polated in time and space to provide hourly boundary conditions for the respective outer domains of the CMAQ and SILAM simulations. The setup for initial and boundary concentrations for EMEP/MSC-W is described in Simpson et al. (2012). ICONs and BCONs are based on long-term observations. For ozone, 3-D fields for the whole domain are specified from climatological ozone sonde datasets, modified monthly against clean-air surface observation. For most other chemical compounds they are

defined by simple functions based on measurements and/or model calculations, prescribing concentrations in terms of latitude and time-of-year, or time-of-day.

2.2.4 Anthropogenic land-based emissions

Anthropogenic land-based emissions in hourly resolution obtained from the SMOKE-EU (Bieser et al., 2011a) emission inventory were provided for CMAQ and SILAM. These emissions are based on officially reported EMEP emissions which are then distributed in time and space using appropriate surrogates like population density maps, street maps or land use maps. Point sources from the European point source emission register are considered. Vertical distribution of point source emissions is based on real-world stack information and calculated within SMOKE-EU (Bieser et al., 2011b). Dynamic emissions from agricultural activity and animal husbandry depending on meteorological variability are considered (Backes et al., 2016). EMEP/MSC-W model uses anthropogenic emissions from the ECLIPSE emission inventory (http://www.iiasa.ac.at/web/home/research/researchPrograms/air/ECLIPSEv5.html). These emissions differ slightly from the reported national total EMEP emissions for 2012, see Wankmüller and Mareckova (2014). For the countries bordering the Baltic Sea (excluding Russia) the national total sulphur emissions from ECLIPSE are about 6 % higher and the NO_2 emissions about 10 % lower than the corresponding EMEP emissions.

2.2.5 Shipping emissions

Shipping emissions for the Baltic Sea and North Sea areas were obtained from STEAM (Jalkanen et al., 2009, 2012; Johansson et al., 2013, 2017). The shipping emissions are used together with the land-based emissions described in Sect. 2.2.4 in all three CTM systems. STEAM uses ship position data of individual ships collected from the AIS base stations network. The AIS data is combined with technical information of the specific vessels and engine types to derive emissions for each individual ship. Shipping emissions are calculated dynamically to consider the emission control areas and regulations, emission abatement equipment on-board the ships as well as fuel sulphur content modelling, separately for main and auxiliary engines (Johansson et al., 2017; Jalkanen et al., 2012).

The STEAM inventory for the Baltic Sea shipping emissions used in the SHEBA project, consist of hourly updated $2 \times 2 \, km^2$ gridded data for NO_X, SO_X, carbon monoxide (CO), and particulate matter, which is further divided into elemental carbon, organic carbon, sulphate (SO_4^{2-}) and mineral ash. For the North Sea and other European seas the STEAM data for 2011 were used. Ship emission were used with hourly time resolution in CMAQ and SILAM whereas they were used with monthly resolution in EMEP/MSC-W.

The use of monthly aggregated ship emissions in EMEP/MSC-W is justified by the fact that the same set of ship emissions from FMI is applied for different meteorological years in the routine application of EMEP modelling and that ship emissions from other seas were only available for 2011. Previous tests with daily and monthly aggregated ship emissions showed that the differences in results are very small. The use of North Sea ship emissions from 2011 on hourly basis in CMAQ and SILAM causes some inconsistency because meteorological data of 2012 is used in the CTM simulations. Because we are

mainly interested in the seasonal variability of pollutant concentrations based on daily averages, the outcome of this study will be less affected by the inconsistency between the timing of ship emissions and the meteorological conditions.

STEAM emission data was provided for two vertical layers (below 36 m, from 36–1000 m). The vertical distribution of STEAM emissions was applied differently in the CTMs (see Table 2). In the CMAQ model, emissions below 36 m were

5 attributed to the lowest vertical model layer, while emissions above 36 m were attributed to the second lowest layer. In the SILAM simulation, the emissions were assumed to be evenly distributed within the emission layers between ground and 1000 m, and were attributed to the model layers accordingly. In EMEP/MSC-W all ship emissions were attributed to the lowest vertical model layer, which typically has a height of 92 m.

2.3 Statistical analysis

10 ### 2.3.1 Evaluation method

Model results for surface concentrations of NO_2, O_3, SO_2, and $PM_{2.5}$ from the three CTMs are evaluated against available measurements of the air quality monitoring network from the AirBase version 8 database (Simoens, 2014). AirBase is the air quality information system maintained by the European Environmental Agency (EEA) through the European topic centre on Air Pollution and Climate Change Mitigation.

15 Table S1 gives a list of all rural and regional background monitoring stations. Concentrations of NO_2 are monitored at 17 stations, O_3 at 35, SO_2 at 11, and $PM_{2.5}$ at 8 rural/regional background stations. Table S2 gives all urban and suburban background monitoring stations included in the statistical evaluation of the models. Concentrations of NO_2, O_3, SO_2, and $PM_{2.5}$ are monitored at 52, 46, 37, and 10 stations of the urban background, respectively. Fig. 2a shows locations of stations with NO_2 and with O_3 measurements. Fig. 2b shows locations of the stations with SO_2 and with $PM_{2.5}$ measurements.

20 The model output of surface concentration fields of each CTM is used with its original horizontal resolution to calculate daily mean concentrations. The modelled concentrations are extracted from the respective model grid cell where the selected monitoring stations are located. The evaluation was done for the entire year 2012 based on daily means. The model output for $PM_{2.5}$ was taken from the modelled $PM_{2.5}$ containing aerosol water at 50 % relative humidity.

The performance of each model is quantified in terms of mean values (μ_{Mod} and μ_{Obs}), normalized mean bias (NMB),

25 Spearman's correlation coefficient (R), root mean square error of the modelled values (RMSE) and fraction of model values within factor 2 of the observations (FAC2). The model performance analysis is discussed separately for rural background stations and urban background stations. In order to better highlight model differences in terms of urban areas and station types (i.e. rural, sub-urban, urban background sites), groups of stations (rural versus urban) are generated in which statistical performance indicators are averaged. In the rural group, rural background and regional background stations are included, while

30 in the urban group, urban background and sub-urban background stations are included. Monitoring stations classified as traffic stations and industrial stations were not included in the comparison, since the regional CTM systems applied here do not handle the local scale dispersion near emission sources.

In the context of this evaluation of predicted air pollutant concentrations, we consider a correlation coefficient of more than 0.5 to indicate a correlation between modelled and observed time series, while values of 0.7 and above are considered as a good correlation. Hanna and Chang (2012) define certain acceptance criteria for model performance based on their experience in conducting a large number of model evaluation exercises. For rural stations FAC2 values > 0.5 and for urban stations FAC2 values > 0.3 indicate acceptable performance. We adopt these bounds in the present study to characterize the predictive strength of the models with respect to the pollutant concentrations.

Further, we compare the performance between models with the help of a graphical comparison in form of boxplots. Boxplots of the correlation coefficient, NMB and RMSE including either all rural or all urban monitoring stations were prepared. The boxplots show the median as line dividing the box in two parts, the upper and lower quartiles as end of the box, the minimum and maximum values of the data and outliers.

2.3.2 Significance of the ship contribution

The method described in Aulinger et al. (2016) was used to assess the significance of ship influence on ambient NO_2 at the monitoring stations. The ship influence at a station was positively confirmed in the tests if: (1) the concentrations increased and (2) the temporal correlation improved, when shipping emissions are included in the CTM simulation.

By means of a paired t-test it was first tested whether the modelled NO_2 concentrations at the monitoring stations with available NO_2 observations (Table S1) significantly increased if shipping emissions were considered. This test estimated whether the mean concentration difference between the "noship" run and the "base" run ("noship" - "base") is significantly equal to or greater than zero, indicated by the probability p_{bias}. If the value of p_{bias} is larger than the level of significance of 0.05, than this hypothesis was confirmed. Otherwise, it was decided that the model run without shipping emissions led to lower concentrations, confirming the ship influence.

The significance of the improvement in the correlation between simulations and observations was tested by calculating the Fisher z transformation of the two correlation coefficients for the two model runs ("noship" and "base") and testing the hypothesis "greater than". Correlation coefficients were calculated with Spearman's method (Myers and Sirois, 2006) for consistency with the statistical evaluation. The probability p_{corr} for the hypothesis that the correlation between the base run and observations is greater than the correlation between the "noship" run and observations was calculated. We accepted this hypothesis if the probability was higher than 0.9. Therefore, in the following, a station i with $p_{corr,i} > 0.9$ for a specific CTM simulation is termed ship-influenced.

3 Results

3.1 Comparison to observations

A statistical performance analysis for each of the three CTMs was undertaken using the available observation data form AirBase for 2012 based on daily mean concentrations. The results of the statistical performance analysis are summarized in Table S3

for daily mean NO_2, in Table S4 for daily mean O_3, in Table S5 for daily mean SO_2 and in Table 3 for daily mean $PM_{2.5}$. In the following, the performance of the models to simulate air pollutant concentrations is compared and discussed separately for the group of rural stations and for the group of urban stations in order to highlight differences in the predictive capability of the models for rural versus urban sites. Moreover, the significance of the ship contribution to the monitored daily mean NO_2 has

5   been tested for the three CTMs. The results of the significance test are summarized in Table S6.

3.1.1   Statistical evaluation for NO_2 at rural and urban sites

Emissions of NO_X from traffic and various combustion sources are mainly in the form of nitrogen oxide (NO) which oxidises to NO_2 within a few minutes through the titration reaction with O_3. NO_2 plays a major role in atmospheric reaction cycles that produce ground-level ozone. NO_2 also contributes to the formation of secondary particulate matter. The atmospheric lifetime

10 of NO_2 is relatively short; a few hours in summer and up to one day in winter (Schaub et al., 2007), hence differences between rural and urban sites are expected due to the higher emission density in urban or industrial areas.

Fig. S1 compares the times series of daily mean NO_2 concentrations from the three CTMs at two rural background stations and at two urban background stations. The seasonal variation at the two rural sites DESH008 (Bornhöved, Germany) and DK0054A (Keldsnor/9054, Denmark) with peak concentrations in winter are captured by the models (Fig. S1a,b). CMAQ

15 shows frequent peaks at the DK0054A during summer. This feature is also seen for other coastal rural sites and could indicate that, due to the high spatial resolution of the model, ship exhaust plumes are resolved but not adequately dispersed. Since the models do not specifically treat the plume dispersion of individual ships, the spreading of the plume might not be sufficiently large or the plume rise of ship exhaust is not properly considered with the applied vertical profile of ship emissions. The other two models also tend to give higher NO_2 than observed at DK0054A in summer. The correlation between predicted and

20 observed daily mean NO_2 for this site is low for all models (R < 0.3). The seasonal variation at the two urban sites DK0053A (Aalborg/8158, Denmark) and LV0RKE2 (Riga Kengarags-2, Latvia) are reproduced by the models, although CMAQ and SILAM underestimate daily mean NO_2 in winter at LV0RKE2 (Fig. S1c,d).

The rural station average of observed annual mean NO_2 is $6.9 \, \mu g \, m^{-3}$ (range: 1.1–$15.8 \, \mu g \, m^{-3}$). The models reproduced the annual means at rural sites very well; modelled annual mean NO_2 is 6.5, 8.1 and $6.0 \, \mu g \, m^{-3}$ for CMAQ, SILAM and

25 EMEP/MSC-W, respectively. The overall correlation of NO_2 for rural stations is good for all models, with R of 0.72, 0.64 and 0.65 for CMAQ, SILAM and EMEP/MSC-W, respectively, as shown in the boxplots in Fig. 3a. At most rural stations the NMB is between -0.5 and 0.5 for all models. An exception is SE066A (Norr Malma, Sweden), where NO_2 is largely overestimated by the models (outlier in the boxplot). This is also the only rural station, for which FAC2 of all models is below 0.5. For SE066A, the influence of traffic emissions from the nearby motorway might be too high in the models, as the spatial resolution is still

30 not fine enough to resolve the dispersion near local sources. The average RMSE at rural sites is 4.7, 5.9 and $3.9 \, \mu g \, m^{-3}$ for CMAQ, SILAM and EMEP/MSC-W, respectively.

The urban station average of observed annual mean NO_2 is $16.7 \, \mu g \, m^{-3}$ (range: 6.7–$34.1 \, \mu g \, m^{-3}$), more than twice the concentration average at rural sites. The three CTMs underestimate the annual means at urban sites (range of model averages: 9.9–$10.9 \, \mu g \, m^{-3}$). The overall correlation of NO_2 for urban sites is lower than at the rural sites, with R between 0.5 and 0.6 for

the models, as shown in the boxplots in Fig. 3b. At most urban stations, models underestimate the observed NO_2 by ca. 40 % (NMB ranges: -0.9–0.1, -0.8–0.2 and -0.8–0.4 for CMAQ, SILAM and EMEP/MSC-W, respectively) (Table S3). For some urban stations the FAC2 is below 0.3, but for the majority of the stations all models fulfil the acceptance criteria for urban sites. The average RMSE at urban sites is 9.9, 10.1 and 9.6 µg m^{-3} for CMAQ, SILAM and EMEP/MSC-W, respectively.

5   The general underestimation of NO_2 at urban sites has been evident in other multi-model air quality studies in Europe (e.g. Giordano et al., 2015). The finer horizontal resolution of CMAQ and SILAM (4 km) compared to EMEP/MSC-W (11 km) does not result in a significant improvement of the urban bias and urban temporal correlation. This result was expected based on the study by Schaap et al. (2015), who found no further improvement of the urban signal, i.e. the concentration difference between high emission areas and their surroundings, when increasing the resolution from 14 km to 7 km in the same model.

10   Moreover, increasing the spatial resolution in the model does not help to improve significantly the performance in time because the temporal variability of pollutants is largely controlled by the meteorological conditions and pollution levels upwind (Schaap et al., 2015).

3.1.2   Statistical evaluation for O_3 at rural and urban sites

Tropospheric ozone is largely controlled by the atmospheric transport from regions outside the study area, by stratosphere-
15   troposphere exchange and by the photochemical production through the oxidation of VOCs and carbon monoxide (CO) in the presence of NO_X and sunlight. Near the surface, the depletion via reaction with NO (titration reaction) in environments with high NO_X levels and dry deposition are important sinks of ozone.

The seasonal variation at the two rural sites DESH008 and DK0054A (same stations as for NO_2) is captured by the models, but high O_3 concentrations in July and August at DK0054A are underestimated by CMAQ and SILAM (Fig. S2a,b). The
20   underestimation of observed ozone in summer by the CMAQ simulation is also found for other coastal stations (Karl et al., 2018) and indicates too low photochemical reactivity. The seasonal variation at the two urban sites DK0053A and LV0RKE2 is captured by the models (Fig. S2c,d). The good performance of the models for O_3 at the urban sites is partly attributed to the high spatial resolution, as NO_X emissions are injected into a smaller grid box volume and consequently less diluted initially. Thus the models are capable of representing the titration effect on the day-to-day variation of ozone.

25   The rural station average of observed annual mean O_3 is 56 µg m^{-3} (range: 44–71 µg m^{-3}). The models show a good correlation with observed O_3 at the rural stations is, with R of 0.74, 0.76 and 0.77 for CMAQ, SILAM and EMEP/MSC-W (Fig. 4a). Modelled daily mean O_3 is in agreement with observed daily mean O_3 within a narrow NMB range for rural sites. CMAQ and SILAM have no bias (average NMB = 0.0), whereas EMEP/MSC-W slightly overestimates the measurements (average NMB = 0.17). The ozone bias might be linked to boundary conditions (Giordano et al., 2015): EMEP/MSC-W uses ozone
30   boundary conditions from long-term observations, whereas CMAQ and SILAM models use boundary conditions from the FMI APTA global reanalysis.

The higher density of NO_X emissions in urban areas is expected to lead to a larger titration effect of NO on ozone, which results in lower average O_3 at the urban sites compared to rural sites. The urban station average of observed annual mean O_3 is 48 µg m^{-3} (range: 38–59 µg m^{-3}). CMAQ and SILAM predict similar annual mean concentrations as observed for both rural

and urban sites, whereas EMEP/MSC-W predicts higher annual mean ozone. As for the rural sites, the models show a good correlation with observed O_3 at the urban stations, with R between 0.73 and 0.77 (Fig. 4b). The models slightly overestimate the O_3 measurements at urban sites, with CMAQ having the smallest bias (average NMB = 0.08).

FAC2 of the models is larger than 0.75 for all rural sites and larger than 0.57 for all urban sites. The average RMSE values
5 for the rural sites and the urban sites, respectively, are similar for the three models (Fig. 4), indicating comparable model performance for the CTMs with respect to daily mean O_3 concentrations.

3.1.3 Statistical evaluation for SO_2 at rural and urban sites

Another major air pollutant is SO_2. It is primarily emitted from anthropogenic emission sources such as coal power plants, residential heating, waste incineration and shipping activities. SO_2 acts as a precursor to sulphates, which are one of the main
10 components of particulate matter in the atmosphere. The atmospheric lifetime of SO_2 is on the order of a few days (Lee et al., 2011). SO_2 can still be considered to be relatively short-lived and thus less influenced by transport from regions outside the study area. Most emission sources of SO_2 are located in urban areas. In the case of power plants, the emissions of SO_2 are however injected at elevated height and therefore do not directly impact the surface concentrations in the urban area. On the other hand, residential heating emissions of SO_2 strongly influence surface concentrations in urban areas during winter. In
15 coastal harbour cities, SO_2 from shipping is a relevant contributor (Viana et al., 2014).

The seasonal variation at the two rural sites SE0001A (Rådhuset, Sweden) and FI00208 (Luuki, Finland; rural) is rather well reproduced by the models (Fig. S3a,b). CMAQ and SILAM overestimate the observed SO_2 concentrations in winter. EMEP/MSC-W underestimates observed SO_2 concentrations at FI00208 and also at other rural stations. The seasonal variation at the two urban sites DESH023 (Lübeck-St. Jürgen, Germany) and LT00044 (Kaunas-Noreikiskes, Lithuania) is captured by
20 the models (Fig. S3c,d). CMAQ and SILAM show too high SO_2 concentrations in winter and EMEP/MSC-W underestimates observed SO_2 during summer.

The rural station average of observed annual mean SO_2 is $1.3\,\mu g\,m^{-3}$ (range: 0.7–$2.5\,\mu g\,m^{-3}$). The annual means of the models at rural sites is in the range of 0.8 to $2.2\,\mu g\,m^{-3}$. With only 10 stations, the rural station group for SO_2 is rather small, limiting the conclusions that can be drawn from the statistical analysis. The model data and the observations for SO_2 at the
25 rural stations are correlated, with R of 0.67, 0.65 and 0.55 for CMAQ, SILAM and EMEP/MSC-W (Fig. 5a). At rural and urban sites, the modelled daily mean SO_2 from CMAQ and SILAM has a positive bias, whereas modelled daily mean SO_2 from EMEP/MSC-W has a slight negative bias. FAC2 of the models is larger than 0.5 for most rural sites. For CMAQ, only one station (EE0016A, Saarejärve, Estonia) does not fulfil the acceptance criteria, due to frequent overestimation of observed SO_2. The average RMSE at rural sites is 1.5, 2.4 and $1.2\,\mu g\,m^{-3}$ for CMAQ, SILAM and EMEP/MSC-W, respectively.

30 At urban stations, the correlation between model data and observed SO_2 shows a mixed performance of the models, with good correlation at some stations and poor correlation at others (Fig. 5b). The urban station average of observed annual mean SO_2 is $3.9\,\mu g\,m^{-3}$ (range: 1.0–$8.0\,\mu g\,m^{-3}$), three times higher than at the rural stations. CMAQ and SILAM predict similar annual mean concentrations, whereas EMEP/MSC-W predicts 36 % lower concentrations for the urban sites. For CMAQ and SILAM, FAC2 is larger than 0.3 for all urban sites. For EMEP/MSC-W some stations have a FAC2 below 0.3, due

to underestimation of observed SO_2. The average RMSE at urban sites is 4.2, 4.3 and 3.3 µg m^{-3} for CMAQ, SILAM and EMEP/MSC-W, respectively.

3.1.4 Statistical evaluation for PM$_{2.5}$ at rural and urban sites

Ambient PM$_{2.5}$ is a wide-spread pollutant, which is directly emitted by biomass and fossil fuel combustion in domestic and
5 industrial activities, and it is also formed from gaseous precursors such as NO_X, SO_2, NH_3 and NMVOC in the atmosphere. The atmospheric lifetime of PM$_{2.5}$ is on the order of days or weeks and thus PM$_{2.5}$ can be subject to long-range transport.

The seasonal variation at the two rural sites SE0001A and FI00208 (same stations as for SO_2) is well reproduced by the models (Fig. S4a,b). CMAQ and EMEP/MSC-W underestimate the observed PM$_{2.5}$ concentrations at SE0001A in summer. The seasonal variation at the two urban sites DESH023 and LT00044 is nicely reproduced by the models (Fig. S4c,d). CMAQ
10 underestimates the observed PM$_{2.5}$ concentrations at both urban stations in summer. This is also found for other stations of the regional background and can partly be attributed to the underestimation of secondary organic aerosols and to the missing emissions of wind-blown soil dust particles in the CMAQ simulation (Karl et al., 2018).

The rural station average of observed annual mean PM$_{2.5}$ is 7.0 µg m^{-3} (range: 3.3–12.6 µg m^{-3}). The modelled annual mean PM$_{2.5}$ is 5.5, 6.7 and 3.8 µg m^{-3} for CMAQ, SILAM and EMEP/MSC-W, respectively. For PM$_{2.5}$ smaller differences
15 between rural and urban stations are expected than for NO_2 and SO_2 because PM$_{2.5}$ has a large secondary component, which is generally more homogeneously distributed over rural and urban areas. The urban station average of observed annual mean PM$_{2.5}$ is 10.5 µg m^{-3} (range: 4.8–13.2 µg m^{-3}) within a similar range as the rural sites. SILAM predicts a similar annual mean for urban stations, whereas CMAQ and EMEP/MSC-W give lower annual mean values.

For rural stations the temporal correlation of PM$_{2.5}$ is slightly better for EMEP/MSC-W than for CMAQ and SILAM
20 (Fig. 6a). For urban stations the temporal correlation of PM$_{2.5}$ is good, with average R between 0.68 and 0.71 (Fig. 6b). At rural and urban sites, the modelled daily mean PM$_{2.5}$ from CMAQ and EMEP/MSC-W has a slightly negative bias, whereas modelled daily mean PM$_{2.5}$ from SILAM has no bias (Table 3).

The average RMSE at the rural sites is between 4.9 and 5.4 µg m^{-3}. It should be noted that RMSE station values for SILAM are within a smaller range (between lower and upper quartile) than the other two models. The performance for urban stations
25 in terms of RMSE is similar for the models, with average RMSE between 6.4 and 7.2 µg m^{-3}.

3.1.5 Significance of ship contribution to NO$_2$ at monitoring stations

A statistical method (Sect. 2.3.2) was applied to decide whether the modelled concentration as well as the correlation with observed NO_2 concentration at a specific station increases significantly when ship emissions are included in the CTM simulation. If both the concentration and the correlation increased, the station is termed ship-influenced. A significant concentration in-
30 crease was found at all 69 stations for CMAQ and EMEP/MSC-W but only at 78 % of the stations for SILAM. However, the significance of the concentration increase only shows that the modelled concentrations at a station are sensitive to ship emissions. The correlation increases significantly (on 0.9 or 0.95 level) at 7, 10, and 11 stations for CMAQ, SILAM and EMEP/MSC-W, respectively (Table S6).

The ship-influenced stations identified by CMAQ included two stations at the shoreline (EE0011R, Vilsandi, Estonia, Fig. S5a; FI00349, Utö, Finland, Fig. S5b), three stations in small harbour cities (DESH023, Lübeck-St. Jürgen; EE0022A, Narva, Estonia; SE0022A, Södermalm, Sweden) and two stations further inland (FI00431, Palokka 2, Finland; PL0077A, KpZielBoryTuch, Poland). Some of these stations (EE0011R, FI00349, FI00431 and PL0077A) were also identified by the

5   other models. The ship influence at station Rostock Warnemünde (DEMV021, Germany), located close to a harbour, was significant in both EMEP/MSC-W and SILAM but not in CMAQ (Fig. S5c). This could indicate that differences in the meteorological data, in particular wind flow fields, are responsible for the different ship influence. Although, the timing and location of ship exhaust plumes - based on AIS data - should be accurate during the port stays, the emission fluxes at berth are more challenging to estimate, because this involves estimation of electrical power usage during the port stays. Station DK0054A

10   (Keldsnor/9054) (Fig. S5d), although close to the shoreline, did not fulfil the correlation criteria, either because the station is not situated downwind of the ship plumes or the models did not properly resolve the ship plumes due to the sub-grid variability of the plume dispersion (see Sect. 3.1.1).

3.2   Comparison of the spatial distribution of air quality indicators

3.2.1   Spatial distribution of annual mean NO_2

15   A strong south-north gradient for annual mean NO_2 concentrations is found for the Baltic Sea region in the three "base" simulations, with 4–5 times higher NO_2 concentrations in the south-western part than in the northern part of the region (Fig. 7a). High modelled NO_2 concentrations are predicted in Denmark, northern Germany, and Poland as well as over the Danish Straits and in the urbanized areas of the region. Modelled annual mean NO_2 concentrations in proximity of the main shipping routes several times exceed the concentrations in the regional background. EMEP/MSC-W shows the strongest concentration

20   gradients between urban and rural areas and between ship lanes and surrounding sea. The simulations with the other two models result in a wider spread of the NO_X emissions from the ship routes and the urban centres, indicating stronger horizontal transport by advection and diffusion in CMAQ and SILAM. This finding is counter-intuitive as the NO_X emissions are initially less diluted than in the EMEP/MSC-W simulation because of the smaller volume of the grid boxes and should therefore result in higher NO_X concentrations near the emission sources.

25   Atmospheric transport by diffusion processes are sub-grid mixing processes, which are not resolved by the given resolution of the applied models. For large grid cells, e.g. $50 \times 50 \, \text{km}^2$, the numerical diffusion will usually be much larger than the physical diffusion in the horizontal direction. However, at finer resolution scales, the physical diffusion will gradually become more important than numerical diffusion and becomes greater than numerical diffusion for $5 \times 5 \, \text{km}^2$ cell size or below (Karl et al., 2014).

30   The wider spread of elevated NO_2 concentrations is also indicative for a longer atmospheric lifetime of NO_2 in CMAQ and SILAM compared to the simulation with EMEP/MSC-W. NO_2 is removed relatively quickly in the lower troposphere through the reaction with hydroxyl (OH) radicals to form HNO_3. The rate coefficient for this reaction, $k(NO_2+OH)$, is similar in the three models $((1.1–1.2)\times10^{-11} \, \text{cm}^3 \, \text{s}^{-1}$ at 298 K$)$. Thus, differences in the NO_2 lifetime are mainly due to different abundances

of OH radicals in the simulations. High NO_2 concentrations in Belarus and Russia in the SILAM simulation are an artefact from merging with the output of the coarser central model grid (Sect. 2.2.1).

3.2.2 Spatial distribution of annual mean O_3

Modelled annual mean O_3 concentrations over the Baltic Sea are 15–25 % higher than over land, but are reduced along the ship lanes due to the titration effect caused by the ship-emitted NO_X (Fig. 7b). Lowest ozone concentrations are seen for St. Petersburg ($< 32\,\mu g\,m^{-3}$) in the three simulations, although we note that the city is outside of the high-resolution grid in the case of SILAM. The spatial average of annual mean O_3 is clearly higher for the EMEP/MSC-W simulation, by 15–25 %, compared to the other two simulations (Table 4). The most probable reason for the difference is the application of different sets of boundary conditions for the European model domains, as discussed in Sect. 3.1.2. Model simulations for Europe have shown a high sensitivity of ozone changes to the dry deposition to vegetation (Andersson and Engardt, 2010). Thus differences in the deposition schemes may partly explain the different O_3 levels over the continent, e.g. when comparing ozone over Sweden and Finland between CMAQ and SILAM.

3.2.3 Spatial distribution of annual mean SO_2

Clear differences in the spatial distribution of the annual mean SO_2 concentrations are found between CMAQ and SILAM on one hand and EMEP/MSC-W on the other hand (Fig. 7c). The simulation with CMAQ and SILAM show a southeast-northwest gradient with elevated SO_2 over large parts of the southern Baltic Sea region, Poland, Belarus, Russia and the Baltic States with annual mean concentrations in the range of $1.3–3.0\,\mu g\,m^{-3}$. Residential heating emissions and power plant emissions for district heating in the urban centres and rural areas strongly contribute to the high SO_2 concentrations in this sub-region. In the EMEP/MSC-W simulation, elevated SO_2 concentrations are present along the main shipping routes, in urban areas and in Poland, whereas the levels of SO_2 outside of these areas are much lower.

The concentration gradients between urban and rural areas and between ship lanes and surrounding sea is up to $2.5\,\mu g\,m^{-3}$ for EMEP/MSC-W while it is only up to $0.7\,\mu g\,m^{-3}$ for CMAQ and SILAM. Factors contributing to the different gradients are differences in the representation of horizontal transport (see Sect. 3.2.1), differences in the meteorological conditions, and differences in the atmospheric lifetime of SO_2. The atmospheric lifetime of SO_2 is determined by its reaction with the OH radical and by its removal via dry deposition. In EMEP/MSC-W, the canopy uptake of SO_2 is strongly controlled by NH_3 levels, and the implemented deposition parameterization accounts for co-deposition effects on the dry deposition of SO_2 (Simpson et al., 2012). Co-deposition effects are not considered in the other two models.

3.2.4 Spatial distribution of annual mean $PM_{2.5}$

Modelled annual mean $PM_{2.5}$ is higher in the southern part, both over land and sea, than in the northern part of the Baltic Sea region (Fig. 7d). On annual average, $PM_{2.5}$ concentrations are not elevated along the ship routes. The seasonal differences between summer and winter will be discussed below (Sect. 3.4) and will help to understand differences between the models.

High $PM_{2.5}$ levels ($8\,\mu g\,m^{-3}$ and higher) are simulated in the urban areas of major cities like Copenhagen, Oslo, Helsinki, Riga, Tallinn and St. Petersburg. The high $PM_{2.5}$ levels over the continent in the southern part of the Baltic Sea region presumably result from a combination of land-based primary emissions, long-range transported particles and the formation of secondary particulate matter.

3.3 Comparison of the ship contribution in the three CTMs

The influence of shipping emissions on the air quality was evaluated for the annual mean concentrations of the three CTMs. The results for the impact of shipping emissions were calculated as differences between the "base" and the "noship" simulations. Results for the absolute ship-related concentrations of O_3, NO_2, SO_2 and $PM_{2.5}$ are shown in Figure 8, the resulting relative ship contribution to annual mean concentrations is shown in Fig. S6 and the spatial average of the relative ship contribution is given in Table 5.

3.3.1 Ship contribution to annual mean NO_2

The ship-related annual mean NO_2 concentrations from the three CTMs are in the range of 3–$5\,\mu g\,m^{-3}$ along the main ship routes. The NO_2 ship contribution decreases to Baltic Sea background values (about $1\,\mu g\,m^{-3}$) within a few hundred kilometres distance from the centre of the shipping routes. Ships emit NO_X mainly in the form of NO, which is however quickly converted to NO_2, thus atmospheric NO_X is mainly in the form of NO_2. The relative contribution of ship emissions to annual mean NO_2 is more than $40\,\%$ over the Baltic Sea (Fig. S6) and 22–$28\,\%$ for the entire Baltic Sea region (Table 5). NO_X emissions from shipping affect the harbour cities of the region and coastal areas in southern Sweden. SILAM predicts the weakest relative ship influence in the Baltic Proper and the Gulf of Finland. Such local differences might be due to the different meteorological drivers or differences in the titration efficiency for ozone.

3.3.2 Ship contribution to annual mean O_3

In the proximity of the main shipping routes, negative concentration differences for the modelled annual mean O_3 between the "base" and the "noship" simulation are obtained as a result of the titration effect by the NO_X emissions from shipping. The highest ozone reduction due to shipping is found in the western part of the Baltic Sea. In the CMAQ simulation the depletion of ozone is stronger than in the other two models; with O_3 reduction by 6–$12\,\mu g\,m^{-3}$ in the Kattegat and in the Danish Straits. The hourly variation of ship emissions is represented in the simulations with CMAQ and SILAM, whereas monthly averaged ship emissions are used in the EMEP/MSC-W simulation. Emission peaks of NO_X from ships that are present in the hourly data can result in occasional stronger ozone titration leading to overall higher reduction of ozone, than it is the case for monthly averaged ship emissions. The SILAM simulation shows only a small influence of shipping on annual mean O_3 along the ship lanes, i.e. the titration effect is much weaker than in the other two models. SILAM shows ozone increases by ca. $2\,\mu g\,m^{-3}$ in a distance of several hundred kilometres from the ship lanes in Baltic Proper, which is not evident for the other models.

This might indicate a NO$_X$-limited regime in some areas of the Baltic Sea, where ozone increases with increasing NO$_X$ from shipping.

3.3.3 Ship contribution to annual mean SO$_2$

Ship emissions of SO$_2$ have a high contribution to annual mean SO$_2$ concentrations over the Baltic Sea. The ship contribution to
SO$_2$ is 0.5–0.7 μg m^{-3} in a wide corridor around the main shipping routes of the Baltic Sea. While the absolute ship contribution of the three CTMs is similar, the relative ship contribution in the EMEP/MSC-W simulation is higher in most areas of the Baltic Sea and in Sweden, because the background atmospheric SO$_2$ levels in this simulation are lower than in CMAQ and SILAM.

3.3.4 Ship contribution to annual mean PM$_{2.5}$

The ship contribution to annual mean PM$_{2.5}$ shows a gradient from southwest to north with highest concentrations over Den-
mark, the west coast of Sweden, the Belt Sea/Kattegat and over the sea south of Sweden with maximum values up to 0.9 μg m^{-3}.
The relative contribution in these ship-impacted areas is up to 10 %. In the entire Baltic Sea region the average contribution is in
the range of 4.3–6.5 % for the three CTMs. The absolute ship contribution in SILAM is smaller than for the other two models,
in particular in the southwest part of the Baltic Sea region (Fig. 8d). A possible explanation for this is the lower dry deposition
of fine aerosols in SILAM, in particular over seawater surfaces (Kouznetsov and Sofiev, 2012). The ship-related PM$_{2.5}$ affects
the coastal areas in the Baltic Sea region, as its influence extends further inland than it is the case for ship-related NO$_2$ or SO$_2$.
This can be attributed to the formation of secondary particulate matter in the ship exhaust plume during its transport away from
the main shipping routes.

3.4 Comparison of PM$_{2.5}$ in summer and autumn

CMAQ and EMEP/MSC-W simulations predict higher seasonal mean concentrations of PM$_{2.5}$ in autumn (average of Septem-
ber, October and November, SON) than in summer (average of June, July and August, JJA), whereas the SILAM simulation
predicts higher PM$_{2.5}$ in summer (Fig. 9a,c; Table S9). The temporal correlation between model data and observations of daily
mean PM$_{2.5}$ for the average of the AirBase stations is slightly better in autumn than in summer (Table S7 and S8). Observed
PM$_{2.5}$ in summer is underestimated strongly by CMAQ (at all stations) and to some extent by EMEP/MSC-W. In autumn all
models are in better agreement with observed PM$_{2.5}$.

In summer, modelled mean PM$_{2.5}$ in the region is much higher in the SILAM simulation (5–8 μg m^{-3} in most parts;
7.4 μg m^{-3} on domain average) than for the other two models (< 4 μg m^{-3}, except for the urban areas). The higher summertime
PM$_{2.5}$ in SILAM is most likely due to more efficient SOA production and different primary emission from wildfires and/or
mineral dust. A previous comparison of the models to PM$_{2.5}$ observations from the EMEP station network in Europe reported
similar seasonal mean concentrations of the SIA components, i.e. nitrate (NO$_3^-$), ammonium (NH$_4^+$) and SO$_4^{2-}$, for the three
CTMs in summer (Prank et al., 2016).

Atmospheric
Chemistry
and Physics
Discussions

The calculated ship contribution from all models is higher in summer than in autumn (Table S9). The simulations reflect the greater importance of shipping activities during summer and their influence on $PM_{2.5}$ levels over the entire Baltic Sea and the coastal areas (Fig. 9b). In particular Denmark and the Swedish west coast is highly impacted in summer, with a ship contribution of 0.5–0.9 µg m^{-3} to ambient $PM_{2.5}$ levels.

5   In autumn, all CTMs predict high levels of $PM_{2.5}$ in the southern part of the Baltic Sea region, exceeding 6 µg m^{-3} . High $PM_{2.5}$ in autumn is typically attributed to stagnant meteorological conditions and higher emissions of primary particulate matter from residential heating and energy production. Modelled $PM_{2.5}$ in Sweden and Finland is higher in SILAM than in the other two models. SILAM overestimates observed $PM_{2.5}$ at the stations in Sweden, Lithuania and Finland in summer (NMB: 0.54 on average) and autumn (NMB: 0.31 on average). In an earlier model comparison, all three models were shown to overestimate

10   NO_3^- and NH_4^+ in autumn; while SILAM also overestimated SO_4^{2-} in autumn (Prank et al., 2016).

The ship contribution in autumn in the southwest part of the region is higher in EMEP/MSC-W compared to the other two models (Fig. 9d), obviously a result from larger secondary formation of particulate matter, as mainly the coastal regions are impacted. The formation of SIA in autumn is favoured by lower temperature and higher humidity compared to summer. Since land-based anthropogenic emissions of NH_3 and NO_2 as well as the ship emissions are the same in CMAQ and SILAM, the

15   lower autumn ship contribution in SILAM is mainly attributed to differences in the schemes for inorganic aerosol formation. The investigation of differences between the SIA formation schemes is, however, beyond the scope of this study.

3.5   Comparison of elemental carbon related to ship emissions

Primary carbonaceous particles emitted from ships are the product of incomplete fuel combustion and consist of a mixture of elemental carbon and non-polar organic carbon. In the STEAM ship emission inventory these are separated into emissions of

20   elemental carbon (EC) and organic carbon (OC). The terms EC and BC are used interchangeably in the models, however both can only be regarded as proxies for the concentration of soot particles (Vignati et al., 2010). Here we are mainly interested in the atmospheric fate of EC from ship emissions, as simulated by the models. EC particles are associated with adverse human health effects (Dockery et al., 1993) and contribute to regional haze and poor visibility (e.g. Odman et al., 2007). The atmospheric lifetime of EC is relatively long; around 6 days in the continental outflow (Park et al., 2005) and 4–8 days on global scale

25   (Vignati et al., 2010), with a large uncertainty due to soot ageing processes and wet deposition (Textor et al., 2006). Therefore the removal by deposition within the study region is expected to be rather limited.

The spatial averages of the EC concentrations ("base" simulation) and the ship-contributed EC concentrations are given in Table 6. The seasonality of ship-related EC predicted by the three CTMs is shown in Fig. 10. The levels of ship-related EC are higher in spring and summer than in autumn and winter due to more intense shipping activities. Therefore the ship contribution

30   peaks in the seasons when ambient EC concentrations are lowest (Table 6; Fig. S7). The highest levels of ship-related EC, in the range of 0.03–0.04 µg m^{-3}, occur along the main shipping routes and in the main ports of the region. On regional average, ships contribute 5–7 % to the annual mean EC (Table 5). SILAM predicts a stronger seasonal variability of the ship-related EC than the other models. In particular, modelled EC ship contribution is spring and winter are lower than for CMAQ and EMEP/MSC-W.

Atmospheric
Chemistry
and Physics
Discussions

Shipping emissions of EC are identical in the three CTMs on a monthly basis. Differences between the models are therefore explained by differences in the meteorological conditions, the treatment of atmospheric transport in the models and the vertical ship emission profiles. In CMAQ and EMEP/MSC-W all ship emissions are injected below 100 m height. The lower surface concentrations of ship-related EC in EMEP/MSC-W can thus be attributed to different atmospheric stability, i.e. more frequent

5 neutral conditions, which dilutes the concentration of the emitted pollutant. The fact that EC is more confined to the shipping routes and shows a limited spatial spreading compared to the other models might also indicate less efficient horizontal diffusion in EMEP/MSC-W.

In SILAM, a vertical ship emission profile that specifically distributes the STEAM emissions from 0 m up to 1000 m above the ground, to mimic the plume rise of ship exhaust (Table 2). This way, typically 38 % of the ship emissions are injected

10 in a height above 500 m in the model. In stable conditions, the boundary layer (BL) height over the Baltic Sea is often at or below 500 m (Svensson et al., 2016; Gryning and Batchvarova, 2002), which would effectively prevent pollutant mass emitted in higher vertical layers to reach the surface layer. Climatological simulations over the Baltic Sea show that there is a strong seasonality in the atmospheric stability over the sea with more than 50 % stable conditions in spring whereas during the other seasons unstable conditions dominate together with occasionally neutral conditions (Svensson et al., 2016). Stable

15 conditions over the Baltic Sea in the SILAM simulation will reduce the quantity of ship emissions that can affect the surface layer concentrations. Thus in SILAM a larger proportion of the ship emissions becomes subject to long-range transport and is exported out of the Baltic Sea region. In winter, SILAM and EMEP/MSC-W ship-related EC is very low and the impacted area has a smaller extent than in the other months (white areas in Fig. 10), indicating faster removal of EC particles than in the CMAQ simulation. Different treatment of the hygroscopicity and ageing processes of EC particles, affecting their wet

20 scavenging, could have contributed to the differences among the models.

3.6 Comparison of oxidised nitrogen deposition

Annual atmospheric deposition of total nitrogen to the Baltic Sea basin has declined by about one third between 1995 ($305\,\mathrm{kt\,y^{-1}}$) and 2015 ($222\,\mathrm{kt\,y^{-1}}$) (Bartnicki et al., 2017). During the two decades, the deposition of oxidised nitrogen (N_{oxi}) decreased by 35 % whereas the deposition of reduced nitrogen (N_{red}), i.e. NH_3 and NH_4^+, decreased by only 12 % (Bartnicki

25 et al., 2017).

Results of the spatial distribution of oxidised nitrogen deposition from the three models were compared (Fig. S8). The annual deposition of N_{oxi} shows a strong gradient from southwest to northeast in the simulation by all models. Deposition of N_{oxi} to the Baltic Proper is larger in SILAM and EMEP/MSC-W ($280–350\,\mathrm{mg(N)\,m^{-2}}$) than in CMAQ ($230–290\,\mathrm{mg(N)\,m^{-2}}$). The companion study by Karl et al. (2018) reports a wide-spread underestimation of the wet deposition of nitrate and ammonium

30 by CMAQ in 2012 compared to observations of the regional background monitoring stations of the EMEP network. The underestimation of nitrogen deposition in CMAQ is likely caused by a combination of too slow oxidative conversion of NO_X to HNO_3, low particulate ammonium from the regional background and underestimation of precipitation in the southern Baltic Sea (Karl et al., 2018).

Atmospheric
Chemistry
and Physics
Discussions

The ship-related annual deposition of oxidised nitrogen is however similar among the models and on average 40–60 mg(N) m^{-2} over the Baltic Sea. The relative contribution of shipping emissions to the deposition of N_{oxi} to the Baltic Sea is 24 % for CMAQ (Karl et al., 2018) and 14–18 % for the other two models. The contribution from ships to the oxidised nitrogen deposition in the Baltic Sea basin for year 2012 in the present study is therefore higher than the previous reported range from 12 to 14 %

5 (Hongisto, 2014) for the period 2008 to 2011. The ship-related contribution to the nitrogen deposition to the Baltic Sea is in the range of 21–23 ktN y^{-1} for the three CTMs of this study (Fig. 11), thus 40–70 % higher than for single years of the Hongisto (2014) study. The higher ship contribution in the present study might partially be due to the inter-annual variation of nitrogen deposition caused by changing meteorological conditions, which is typically in the range of -13 % to 17 % (Hongisto, 2014). Most of northern Europe experienced above-average precipitation during 2012; in Finland the annual precipitation in 2012 was

10 739 mm, which is 173 mm above the 1961–1990 average (WMO, 2013). The Hongisto (2014) study applied the STEAM ship emission inventory and fine resolution grids (0.068 degrees), however the specific treatment of SIA formation or the abundance of atmospheric oxidants and NH$_3$ represent possible explanations for the discrepancy.

The total nitrogen deposition to the Baltic Sea when all emissions are considered is ∼230 ktN y^{-1} for EMEP/MSC-W and SILAM, comparable to the estimate of 223.6 ktN y^{-1} (2012; normalised by inter-annual changes in meteorological conditions)

15 used in the HELCOM evaluation of the Baltic Sea marine environmental status (Bartnicki et al., 2017) which uses the EMEP model with the coarser 50 km-resolution. CMAQ computes lower deposition totals: N_{oxi} is 25 % lower and N_{red} is 40 % lower compared to the other two models (Fig. 11). According to the SILAM simulation, wet deposition has a share of 60 % and 66 %, respectively, to the total deposition of N_{oxi} and N_{red} to the Baltic Sea. The wet deposition share was similar in the EMEP simulation but lower in the CMAQ simulation (N_{oxi}: 54 %; N_{red}: 63 %). For SILAM and EMEP/MSC-W, the wet deposition

20 share to total nitrogen deposition is within the range of 63–70 % given for the years 1995–2006 (Bartnicki et al., 2011).

4 Summary and conclusions

The effect of ship emissions on the regional air quality and nitrogen deposition in the Baltic Sea region was investigated with three regional CTM systems (CMAQ, EMEP/MSC-W and SILAM) that simulate the transport, chemical transformation and fate of atmospheric pollutants. The models were applied with their typical setup for air quality studies in European regions. The

25 use of three different CTM systems has the advantage of providing the necessary information for assessing the uncertainties connected with the atmospheric transport and transformation of pollutants. The same ship emission dataset from the STEAM model based on ship movements from AIS records, detailed ship characteristics and up-to-date load dependent emission factors were used in all CTMs. The models were set up with a finer grid resolution (4-km to 11-km grid length) than it was the case for previous air quality studies in the Baltic Sea region, potentially enabling a better treatment of the dispersion and photochemistry

30 in exhaust plumes from shipping along the major ship lanes of the Baltic Sea.

The comparison of air concentrations of regulatory air pollutants among the models is the primary focus of this study. Results from the three CTMs were compared to observations from rural and urban background stations of the AirBase monitoring network in the coastal areas of the Baltic Sea region. The performance of the models to predict pollutant concentrations was

found to be similar. The finer resolution of CMAQ and SILAM (4 km) compared to EMEP/MSC-W (11 km) did not lead to a significant improvement of the urban bias and urban temporal correlation for daily mean NO_2 concentrations. The benefit from using high-resolution grids depends on the availability of accurate urban emission data with high spatial resolution (Schaap et al., 2015) and realistic temporal profiles (Kukkonen et al., 2012). While the STEAM inventory provides this data for

5   shipping, the compilation of urban emission inventories is more challenging because they are based on specific information for each sector, such as housing units for domestic heating or number of vehicles (Guevara et al, 2016). Observed $PM_{2.5}$ in summer is underestimated strongly by CMAQ at all stations and to some extent by EMEP/MSC-W. In autumn all models are in better agreement with observed $PM_{2.5}$. The low summer $PM_{2.5}$ in CMAQ has been attributed to the underestimation of secondary organic aerosols and to the missing emissions of wind-blown soil dust particles (Karl et al., 2018). Particulate matter emissions

10 from wind-blown dust and forest fires are included in EMEP/MSC-W and SILAM.

The ship influence on NO_2 concentrations at coastal monitoring stations was investigated with a statistical method. A station is regarded as ship-influenced if the modelled concentration as well as the correlation with observed NO_2 increased significantly (on 0.9 level or higher) when ship emissions are included in the CTM simulation. Ship-influenced stations identified by the models are mainly located close to the shoreline or close to a port; but a few inland stations up to 200 km distant from the shore

15 were also found to be influenced from shipping. However, modelled peaks of high daily mean NO_2 at coastal rural sites during summer that are not present in the measurements indicate that the models often did not properly resolve the ship plumes due to the sub-grid variability of the plume dispersion of individual ships.

The spatial average of annual mean O_3 concentrations in the EMEP/MSC-W simulation is 15–25 % higher compared to the other two simulations. EMEP/MSC-W overestimates the measurements of daily mean O_3 concentrations at rural stations by

20 17 % on average. The higher ozone concentrations in the EMEP model are mainly the consequence of using a different set of boundary conditions for the European model domain. The concentration gradients of NO_2 and SO_2 between urban and rural areas and between ship lanes and the surrounding sea are larger in EMEP/MSC-W than in the other models. Factors contributing to the different gradients are differences in the representation of horizontal transport, differences in the meteorological driving data, and differences in the atmospheric lifetime of NO_2 and SO_2 in the models.

25 There are significant differences in the calculated ship contributions to the levels of air pollutants among the three models. In the proximity of the main shipping routes, ozone is depleted as a result of the titration effect by NO emissions from shipping. SILAM predicted a much weaker titration effect than the other two models. In contrast with the other models, SILAM shows ozone increases due to shipping several hundred kilometres away from the shipping lanes in the Baltic Proper. The ship-related $PM_{2.5}$ affects the coastal areas in the Baltic Sea region, as its influence extends further inland than it is the case for ship-related

30 NO_2 and SO_2. In the entire Baltic Sea region the average contribution of ships to levels of $PM_{2.5}$ is in the range of 4.3–6.5 % for the three CTMs. Differences in ship-related $PM_{2.5}$ among the models are mainly attributed to differences in the schemes for inorganic aerosol formation.

Since shipping emissions of elemental carbon are identical in the three CTMs on a monthly basis, differences for ship-related EC can be explained by differences in the meteorological conditions, the treatment of atmospheric transport in the models and

the vertical ship emission profiles. In SILAM a large proportion of the ship emissions is injected in altitudes above 500 m and becomes subject to long-range transport out of the Baltic Sea region.

The ship-related annual deposition of oxidised nitrogen is similar among the models. The annual oxidised nitrogen deposition from ships to the Baltic Sea is on average 40–60 mg(N) m^{-2} and annual totals are in the range of 21–23 ktN y^{-1}, and thus higher than previous estimates. The higher ship contribution in the present study might partly be a result of the high precipitation during 2012.

Results obtained from the use of three CTMs give a more robust estimate of the ship contribution to atmospheric concentrations and deposition than a single model. By using several models the sensitivity of the ship contribution to uncertainties of boundary conditions, meteorological data as well as aerosol formation and deposition schemes is taken into account. This is an important step towards a more reliable evaluation of policy options regarding emission regulations for ship traffic and the introduction of a nitrogen emissions control area (NECA) in the Baltic Sea and the North Sea in 2021. In order to improve the calculation of the ship emission influence on local and regional air quality further, better constraints for the vertical emission profile from ships are needed. The plume rise from moving ships should be studied under atmospheric stability conditions relevant in the European seas with the aim to derive generally applicable parameterisations for the vertical profile.

Author contributions.

Matthias Karl: overall structure; CMAQ simulations; evaluation of the air concentration data from all models; framework for statistical processing; visualisation and plotting; main writing tasks

Jan Eiof Jonson: Simulations with the EMEP/MSC-W model; model data provision; text contributions

Andreas Uppstu: SILAM simulations; model data provision; model description

Armin Aulinger: statistical method for ship contribution; R-Scripts for visualisation and data processing

Marje Prank: SILAM simulations; discussions of model results

Jukka-Pekka Jalkanen: shipping emissions with STEAM; text contributions

Lasse Johansson: shipping emissions with STEAM

Markus Quante: development of research questions; discussions of the manuscript structure; text contributions to the introduction, conclusions and the abstract

Volker Matthias: development of research questions; coordination of the intercomparison

Competing interests. The authors declare that they have no conflict of interest

Atmospheric
Chemistry
and Physics
Discussions

Open Access

EGU

Atmospheric
Chemistry
and Physics
Discussions

References

Andersson, C. and Engardt, M.: European ozone in a future climate: Importance of changes in dry deposition and isoprene emissions, J. Geophys. Res.-Atmos., 115, D02303, doi:10.1029/2008JD011690, 2010.

Angelbratt, J., Mellqvist, J., Simpson, D., Jonson, J. E., Blumenstock, T., Borsdor, T., Duchatelet, P., Forster, F., Hase, F., Mahieu, E., De Mazière, M., Notholt, J., Petersen, A. K., Raalski, U., Servais, C., Sussmann, R., Warneke, T., and Vigouroux, C.: Carbon monoxide (CO) and ethane (C_2H_6) trends from ground-based solar FTIR measurements at six European stations, comparison and sensitivity analysis with the EMEP model, Atmos. Chem. Phys., 11(17), 9253–9269, 2011.

Andersson-Sköld, Y. and Simpson, D.: Comparison of the chemical schemes of the EMEP MSC-W and the IVL photochemical trajectory models, Atmos. Environ., 33, 1111–1129, 1999.

Antturi, J., Hänninen, O., Jalkanen, J.-P., Johansson, L., Prank, M., Sofiev, M., and Ollikainen, M.: Costs and benefits of low-sulphur fuel standard for Baltic Sea shipping, J. Environ. Manag., 184, 431–440, 10.1016/j.jenvman.2016.09.064, 2016.

Amann, M., Borken-Kleefeld, J., Cofala, J., Heyes, C., Klimont, Z., Rafaj, P., Purohit, P., Schoepp, W. and Winiwarter, W.: Future emissions of air pollutants in Europe - Current legislation baseline and the scope for further reductions. TSAP Report #1, International Institute for Applied Systems Analysis, Laxenburg, Austria, 2012.

Amann, M., Klimont, Z., and Wagner, F.: Regional and Global Emissions of Air Pollutants: Recent Trends and Future Scenarios. Annu. Rev. Environ. Resour., 38(1), 31–55, 2013.

Appel, K. W., Pouliot, G. A., Simon, H., Sarwar, G., Pye, H. O. T., Napelenok, S. L., Akhtar, F., and Roselle, S. J.: Evaluation of dust and trace metal estimates from the Community Multiscale Air Quality (CMAQ) model version 5.0, Geosci. Model Dev., 6, 883–899, doi:10.5194/gmd-6-883-2013, 2013.

Appel, K. W., Napelenok, S., Foley, K. M., Pye, H. O. T., Hogrefe, C., Luecken, D. J., Bash, J. O., Roselle, S. J., Pleim, J. E., Foroutan, H., Hutzell, W., Pouliot, G., Sarwar, G., Sarwar, G., Fahey, K., Gantt, B., Gilliam, R. C., Kang, D., Mathur, R., Schwede, D., Spero, T., Wong, D. C., and Young, J.: Description and evaluation of the Community Multiscale Air Quality (CMAQ) modeling system version 5.1, Geosci. Model Dev., 10, 1703–1732, doi:10.5194/gmd-10-1703-2017, 2017.

Aulinger, A., Matthias, V., Zeretzke, M., Bieser, J., Quante, M., and Backes, A.: The impact of shipping emissions on air pollution in the greater North Sea region - Part 1: Current emissions and concentrations, Atmos. Chem. Phys., 16, 739–758, doi:10.5194/acp-16-739-2016, 2016

Backes, A., Aulinger, A., Bieser, J., Matthias, V., and Quante, M.: Ammonia emissions in Europe, part I: Development of a dynamical ammonia emission inventory, Atmos. Environ., 131, 55–66, 2016.

Bartnicki, J., Semeena, V. S., and Fagerli, H.: Atmospheric deposition of nitrogen to the Baltic Sea in the period 1995-2006, Atmos. Chem. Phys., 11, 10057–10069, doi:10.5194/acp-11-10057-2011, 2011.

Bartnicki, J., Gauss, M., and Jonson, J. E.: Atmospheric nitrogen depositions to the Baltic Sea during 1995-2015, HELCOM Baltic Sea Environment Fact Sheet, available online at: http://helcom.fi/baltic-sea-trends/environment-fact-sheets/eutrophication/nitrogen-atmospheric-deposition-to-the-baltic-sea/, (Last Accessed 03.09.2018), 2017.

Bergström, R., Denier van der Gon, H. A. C., Prévôt, A. S. H., Yttri, K. E., and Simpson, D.: Modelling of organic aerosols over Europe (2002-2007) using a volatility basis set (VBS) framework: application of different assumptions regarding the formation of secondary organic aerosol, Atmos. Chem. Phys., 12, 8499–8527, doi:10.5194/acp-12-8499-2012, 2012.

Bieser, J., Aulinger, A., Matthias, V., Quante, M., and Builtjes, P.: SMOKE for Europe - adaptation, modification and evaluation of a comprehensive emission model for Europe, Geosci. Model Dev., 4, 47–68, https://doi.org/10.5194/gmd-4-47-2011, 2011a.

Bieser, J., Aulinger, A., Matthias, V., Quante, M., and Denier van der Gon, H. A. C.: Vertical emission profiles for Europe based on plume rise calculations, Environ. Pollut., 159, 2935–2946, https://doi.org/10.1016/j.envpol.2011.04.030, 2011b.

5 Binkowski, F. S. and Roselle, S. J.: Models-3 Community Multiscale Air Quality (CMAQ) model aerosol component 1. Model description, J. Geophys. Res.-Atmos., 108, 4183, doi:10.1029/2001JD001409, 2003.

Binkowski, F. S. and Shankar, U.: The Regional Particulate Matter Model: 1. Model description and preliminary results, J. Geophys. Res.-Atmos., 100, 26,191–26,209, doi:10.1029/95JD02093, 1995.

Byun, D. and Schere, K.: Review of the Governing Equations, Computational Algorithms, and Other Components of the Models-3 Commu-
10   nity Multiscale Air Quality (CMAQ) Modeling System, Applied Mechanics Reviews, 59, 51–77, 2006.

Carlton, A. G., Bhave, P. V., Napelenok, S. L., Edney, E. D., Sarwar, G., Pinder, R. W., Pouliot, G. A., and Houyoux, M.: Model representation of secondary organic aerosol in CMAQ v4.7, Environ. Sci. Technol., 44, 8553–8560, doi:10.1021/es100636q, 2010.

Cofala, J., Amann, M., Heyes, C., Klimont, Z., Posch, M., Schöpp, W., Tarasson, L., Jonson, J., Whall, C., and Stavrakaki, A.: Final Report: Analysis of Policy Measures to Reduce Ship Emissions in the Context of the Revision of the National Emissions Ceilings Directive, March
15   2007, International Institute for Applied Systems Analysis, Laxenburg, Austria, pp. 74, 2007.

Colette, A., Granier, C., Hodnebrog, Ø., Jacobs, H., Maurizi, A. , Nyíri, A., Bessagnet, B., D'Angiola, A., D'Isidoro, M., Gauss, M., Meleux, F., Memmesheimer, M., Mieville, A., Rouïl, L., Russo, F., Solberg, S., Stordal, F., and Tampieri, F.: Air quality trends in Europe over the past decade: a first multi-model assessment, Atmos. Chem. Phys., 11, 11657–11678, doi:10.5194/acp-11-11657-2011, 2011.

Colette, A., Granier, C., Hodnebrog, Ø., Jacobs, H., Maurizi, A., Nyíri, A., Rao, S., Amann, M., Bessagnet, B., D'Angiola, A., D'Isidoro,
20   Gauss, M., Heyes, C., Klimont, Z., Meleux, F., Memmesheimer, M., Mieville, A., Rouïl, L., Russo, F., Schucht, S., Simpson, D., Stordal, F., Tampieri, F., and Vrac, M.: Future air quality in Europe: a multi-model assessment of projected exposure to ozone, Atmos. Chem. Phys., 12(21), 10613–10630, doi:10.5194/acp-12-10613-2012, 2012.

Corbett, J. J., Winebrake, J. J., Green, E. H., Kasibhatla, P., Eyring, V., and Lauer, A.: Mortality from ship emissions: a global assessment. Environ. Sci. Technol., 41 (24), 8512–8518, 2007.

25 Claremar, B., Haglund, K., and Rutgersson, A.: Ship emissions and the use of current air cleaning technology: contributions to air pollution and acidification in the Baltic Sea, Earth Syst. Dynam., 8, 901–919, https://doi.org/10.5194/esd-8-901-2017, 2017.

Dockery, D. W., Pope III, C. A., Xu, X., Spengler, J. D., Ware, J. H., Fay, M . E., Ferris Jr., B. G., and Speizer, F. E.: An association between air pollution and mortality in six U.S. cities, N. Engl. J. Med., 329(24), 1753–1759, doi:10.1056/NEJM199312093292401, 1993.

Donahue, N. M., Epstein, S. A., Pandis, S. N., and Robinson, A. L.: A two-dimensional volatility basis set: 1. organic-aerosol mixing thermo-
30   dynamics, Atmos. Chem. Phys., 11, 3303–3318, 2011.

Dore, A. J., Carslaw, D. C., Braban, C., Cain, M., Chemel, C., Conolly, C., Derwent, R. G., Griffiths, S. J., Hall, J., Hayman, G., Lawrence, S., Metcalfe, S. E., Redington, A., Simpson, D., Sutton, M. A., Sutton, P., Tang, Y. S., Vieno, M., Werner, M., and Whyatt, J. D.: Evaluation of the performance of different atmospheric chemical transport models and intercomparison of nitrogen and sulphur deposition estimates for the UK, Atmos. Environ., 119, 131–143, 2015.

35 EMEP: The EMEP/MSC-W Model - User's Guide, version rv4.8, October 2015, 2015. Available at: https://github.com/metno/emep-ctm/releases/tag/rv4_8 (Last Accessed 01.11.2018), 2015.

Endresen, Ø., Sørgård, E., Sundet, J. K., Dalsøren, S. B., Isaksen, I. S., Berglen, T. F., and Gravir, G.: Emission from international sea transportation and environmental impact, J Geophys. Res., Atmospheres (1984–2012), 108(D17), 4560, doi:10.1029/2002JD002898, 2003.

Eyring, V., Isaksen, I., Berntsen, T., Collins, W., Corbett, J., Endresen, Ø., Grainger, R., Moldanová, J., Schlager, H., and Stevenson, D.: Transport impacts on atmosphere and climate: shipping, Atmos. Environ., 44, 4735–4771, 2010.

EUROSTAT, Maritime transport statistics - short sea shipping of goods, available at: https://ec.europa.eu/eurostat/statistics-explained/index.php/Maritime_transport_statistics_-_short_sea_shipping_of_goods, (Last Accessed 19.10.2018), 2018.

5 Foley, K. M., Roselle, S. J., Appel, K. W., Bhave, P. V., Pleim, J. E., Otte, T. L., Mathur, R., Sarwar, G., Young, J. O., Gilliam, R. C., Nolte, C. G., Kelly, J. T., Gilliland, A. B., and Bash, J. O.: Incremental testing of the Community Multiscale Air Quality (CMAQ) modeling system version 4.7, Geosci. Model Dev., 3, 205–226, doi:10.5194/gmd-3-205-2010, 2010.

Fountoukis, C. and Nenes, A.: ISORROPIA II: a computationally efficient thermodynamic equilibrium model for K^+-Ca^{2+}-Mg^{2+}-NH_4^+-Na^+-SO_4^{2-}-NO_3^--Cl^--H_2O aerosols, Atmos. Chem. Phys., 7, 4639–4659, doi:10.5194/acp-7-4639-2007, 2007.

10 Fridell, E., Steen, E., and Peterson, K.: Primary particles in ship emissions, Atmos. Environ., 42, 1160–1168, 2008.

Giordano, L., Brunner, D., Flemming, J., Hogrefe, C., Im, U., Bianconi, R., Badia, A., Balzarini, A., Baró, R., Chemel, C., Curci, G., Forkel, R., Jiménez-Guerrero, P., X Hirtl, M., Hodzic, A., Honzak, L., Jorba, O., Knote, C., Kuenen, J. J. P., Makar, P. A., Manders-Groot, A., Neal, L., Pérez, J. L., Pirovano, G., Pouliot, G., San José, R., Savage, N., Schröder, W., Sokhi, R S., Syrakov, D., Torian, A., Tuccella, P., Werhahn, J., Wolke, R., Yahya, K., Žabkar, R., Zhang, Y., and Galmarini, S., Assessment of the MACC reanalysis and
15 its influence as chemical boundary conditions for regional air quality modeling in AQMEII-2, Atmos. Environ., 115, 371–388, doi:10.1016/j.atmosenv.2015.02.034, 2015.

Gauss, M., Tsyro, S., Benedictow, A. C., Hjellbrekke, A.-G., and Solberg, S.: EMEP/MSC-W Model Performance for Acidifying and Eutrophying Components, Photo-Oxidants and Particulate Matter in 2013, Supplementary Material to the EMEP Status Report 1/2015, Norwegian Meteorological Institute (EMEP/MSC-W), Oslo, Norway, 1–96, 2015.

20 Gong, S. L.: A parameterization of sea-salt aerosol source function for sub- and super-micron particles, Global Biogeochem. Cy., 17, 1097, doi:10.1029/2003GB002079, 2003.

Gryning, S.-E. and Batchvarova, E.: Marine boundary layer and turbulent fluxes over the Baltic Sea: measurements and modelling, Boundary-Layer Meteorology, 103, 29–47, 2002.

Guevara, M., Lopez-Aparicio, S., Cuvelier, C., Tarrason, L., Clappier, A ., and Thunis, P.: A benchmarking tool to screen and compare bottom
25 up and top-down atmospheric emission inventories, Air Qual. Atmos. Health, 10, 627–642, https://doi.org/10.1007/s11869-016-0456-6, 2016.

Hanna, S. and Chang, J.: Acceptance criteria for urban dispersion model evaluation, Meteorol. Atmos. Phys., 116, 133–146, doi:10.1007/s00703-011-0177-1, 2012.

HELCOM: Eutrophication in the Baltic Sea - An integrated thematic assessment of the effects of nutrient enrichment and eutrophication in
30 the Baltic Sea region. Balt. Sea Environ. Proc., 115B, 1–152, 2009.

HELCOM: Annual report on shipping accidents in the Baltic Sea area during 2012, HELCOM - Baltic Marine Environment Protection Commission, Helsinki, Finland, 43 pp., 2014.

Hettelingh, J.-P., Posch, M., and Slootweg, J.: European critical loads: database, biodiversity and ecosystems at risk, CCE Final Report 2017, Coordination Centre for Effects, RIVM Report 2017-0155, National Institute for Public Health and the Environment, Bilthoven, The
35 Netherlands, 2017.

Hongisto, M.: Impact of the emissions of international sea traffic on airborne deposition to the Baltic Sea and concentrations at the coastline, Oceanologia, 56 (2), 349–372, doi:10.5697/oc.56-2.349, 2014.

Hunter, K. A., Liss, P. S., Surapipith, V., Dentener, F., Duce, R., Kanakidou, M., Kubilay, N., Mahowald, N., Okin, G., Sarin, M., Uematsu, M., and Zhu, T.: Impacts of anthropogenic SO_X, NO_X and NH_3 on acidification of coastal waters and shipping lanes, 38, L13602, doi:10.1029/2011GL047720, 2011.

IMO: The International Convention for the Prevention of Marine Pollution from Ships, 1973 as modified by the Protocol of 1978 relating thereto (MARPOL 73/78), Annex VI: Prevention of Air Pollution from Ships, 2008 Amendments, International Maritime Organization, 2008a.

Jalkanen, J.-P., Brink, A., Kalli, J., Pettersson, H., Kukkonen, J., and Stipa, T.: A modelling system for the exhaust emissions of marine traffic and its application in the Baltic Sea area, Atmos. Chem. Phys., 9, 9209–9223, https://doi.org/10.5194/acp-9-9209-2009, 2009.

Jalkanen, J.-P., Johansson, L., Kukkonen, J., Brink, A., Kalli, J., and Stipa, T.: Extension of an assessment model of ship traffic exhaust emissions for particulate matter and carbon monoxide, Atmos. Chem. Phys., 2641–2659, https://doi.org/10.5194/acp-12-2641-2012, 2012.

Johansson, L., Jalkanen, J.-P., Kalli, J., and Kukkonen, J.: The evolution of shipping emissions and the costs of regulation changes in the northern EU area, Atmos. Chem. Phys., 13, 11375–11389, https://doi.org/10.5194/acp-13-11375-2013, 2013.

Johansson, L., Jalkanen, J.-P., and Kukkonen, J.: Global assessment of shipping emissions in 2015 on a high spatial and temporal resolution. Atmos. Environ., 167, 403–415, doi:10.1016/j.atmosenv.2017.08.042, 2017.

Jonson, J. E., Simpson, D., Fagerli, H., and Solberg, S.: Can we explain the trends in European ozone levels?, Atmos. Chem. Phys., 6, 51–66, doi:10.5194/acp-6-51-2006, 2006.

Jonson, J. E., Tarrason, L., Klein, H., Vestreng, V., Cofala, J., and Whall, C.: Effects of ship emissions on European ground level ozone in 2020, Int. J. Remote Sens., 30, 4099–4110, https://doi.org/10.1080/01431160902821858, 2009.

Jonson, J. E., Stohl, A., Fiore, A. M., Hess, P., Szopa, S., Wild, O., Zeng, G., Dentener, F. J., Lupu, A., Schultz, M. G., Duncan, B. N., Sudo, K., Wind, P., Schulz, M., Marmer, E., Cuvelier, C., Keating, T., Zuber, A., Valdebenito, A., Dorokhov, V., De Backer, H., Davies, J., Chen, G. H., Johnson, B., Tarasick, D. W., Stübi, R. , Newchurch, M. J., von der Gathen, P., Steinbrecht, W., and Claude, H.: A multi-model analysis of vertical ozone profiles, Atmos. Chem. Phys., 10, No. 12, 5759–5783, 2010.

Jonson, J. E., Jalkanen, J. P., Johansson, L., Gauss, M., and Denier van der Gon, H. A. C.: Model calculations of the effects of present and future emissions of air pollutants from shipping in the Baltic Sea and the North Sea, Atmos. Chem. Phys., 15, 783–798, doi:10.5194/acp-15-783-2015, 2015.

Jonson, J. E., Gauss, M., Schulz, M. and Nyíri, A.: Effects of international shipping, In: Transboundary particulate matter, photo-oxidants, acidifying and eutrophying components. EMEP Status Report 1/2018, Norwegian Meteorological Institute (EMEP/MSC-W), Oslo, Norway, 1–204, 2018a.

Jonson, J. E., Schulz, M., Emmons, L., Flemming, J., Henze, D., Sudo, K., Tonstad Lund, M., Lin, M., Benedictow, A., Koffi, B., Dentener, F., Keating, T., Kivi, R. and Davila, Y.: The effects of intercontinental emission sources on European air pollution levels Atmos. Chem. Phys., 18, 13655–13672, doi:.10.5194/acp-18-13655-2018, 2018b.

Karl, M., Castell, N., Simpson, D., Solberg, S., Starrfelt, J., Svendby, T., Walker, S.-E., and Wright, R. F.: Uncertainties in assessing the environmental impact of amine emissions from a CO_2 capture plant, Atmos. Chem. Phys., 14, 8533–8557, https://doi.org/10.5194/acp-14-8533-2014, 2014.

Karl, M., Bieser, J., Geyer, B., Matthias, V., Jalkanen, J.-P., Johansson, L., and Fridell, E.: Impact of a nitrogen emission control area (NECA) on the future air quality and nitrogen deposition to seawater in the Baltic Sea region, Atmos. Chem. Phys. Discuss, acp-2018-2017, in review, 2018.

Kelly, J. T., Bhave, P. V., Nolte, C. G., Shankar, U., and Foley, K. M.: Simulating emission and chemical evolution of coarse seasalt particles in the Community Multiscale Air Quality (CMAQ) model, Geosci. Model Dev., 3, 257–273, doi:10.5194/gmd-3-257-2010, 2010.

Kouznetsov, R. and Sofiev, M.: A methodology for evaluation of vertical dispersion and dry deposition of atmospheric aerosols, J. Geophys. Res. Atmos., 117, D01202, doi:10.1029/2011JD016366, 2012.

5 Kouznetsov, R. and Sofiev, M.: A New Wet Deposition Module in SILAM Chemical Transport Model, American Geophysical Union, Fall Meeting 2013, abstract id. A51G-0117, 2013.

Kukkonen, J., Olsson, T., Schultz, D. M., Baklanov, A., Klein, T., Miranda, A. I., Monteiro, A., Hirtl, M., Tarvainen, V., Boy, M., Peuch, V.-H., Poupkou, A., Kioutsioukis, I., Finardi, S., Sofiev, M., Sokhi, R., Lehtinen, K. E. J., Karatzas, K., San José, R., Astitha, M., Kallos, G., Schaap, M., Reimer, E., Jakobs, H., and Eben, K.: A review of operational, regional-scale, chemical weather forecasting models in Europe, Atmos. Chem. Phys., 12(1), 1-87, https://doi.org/10.5194/acp-12-1-2012, 2012.

Langner, J., Engardt, M., Baklanov, A., Christensen, J. H., Gauss, M., Geels, C., Hedegaard, G. B., Nuterman, R., Simpson, D., Soares, J., Sofiev, M., Wind, P., and Zakey, A.: A multi-model study of impacts of climate change on surface ozone in Europe, Atmos. Chem. Phys., 12, 10423–10440, https://doi.org/10.5194/acp-12-10423-2012, 2012.

Lee, C., Martin, R. V., van Donkelaar, A., Lee, H., Dickerson, R. R., Hains, J. C., Krotkov, N., Richter, A., Vinnikov, K., and Schwab, J. J.: SO_2 emissions and lifetimes: estimates from inverse modeling using in situ and global, space-based (SCIAMACHY and OMI) observations, J. Geophys. Res. Atmos., 116, D6, http://dx.doi.org/10.1029/2010JD014758, 2011.

Marécal, V., Peuch, V.-H., Andersson, C., Andersson, S., Arteta, J., Beekmann, M., Benedictow, A., Bergström, R., Bessagnet, B., Cansado, A., Chéroux, F., Colette, A., Coman, A., Curier, R. L., Denier van der Gon, H. A. C., Drouin, A., Elbern, H., Emili, E., Engelen, R. J., Eskes, H. J., Foret, G., Friese, E., Gauss, M., Giannaros, C., Guth, J., Joly, M., Jaumouillé, E., Josse, B., Kadygrov, N., Kaiser, J. W., Krajsek, K., Kuenen, J., Kumar, U., Liora, N., Lopez, E., Malherbe, L., Martinez, I., Melas, D., Meleux, F., Menut, L., Moinat, P., Morales, T., Parmentier, J., Piacentini, A., Plu, M., Poupkou, A., Queguiner, S., Robertson, L., Rouïl, L., Schaap, M., Segers, A., Sofiev, M., Tarasson, L., Thomas, M., Timmermans, R., Valdebenito, Á., van Velthoven, P., van Versendaal, R., Vira, J., and Ung, A.: A regional air quality forecasting system over Europe: the MACC-II daily ensemble production, Geosci. Model Dev., 8, 2777–2813, https://doi.org/10.5194/gmd-8-2777-2015, 2015.

25 Matthias, V., Bewersdorff, I., Aulinger, A., and Quante, M.: The contribution of ship emissions to air pollution in the North Sea regions, Environmental Pollution, 158, 2241–2250, doi:10.1016/j.envpol.2010.02.013, 2010.

Matthias, V., Aulinger, A., Backes, A., Bieser, J., Geyer, B., Quante, M. and Zeretzke, M.: The impact of shipping emissions on air pollution in the greater North Sea region - Part 2: Scenarios for 2030, Atmos. Chem. Phys., 16, 759–776, doi:10.5194/acp-16-759-2016, 2016.

Moldanová, J., Fridell, E., Popovicheva, O., Demirdjian, B., Tishkova, V., Faccinetto, A., and Focsa, C.: Characterisation of particulate matter and gaseous emissions from a large ship diesel engine, Atmos. Environ., 43, 2632–2641, https://doi.org/10.1016/j.atmosenv.2009.02.008, 2009.

Myers, L. and Sirois, M. J.: Spearman Correlation Coefficients, Differences between, In: Encyclopedia of Statistical Sciences, Eds.: Kotz, S., Read, C. B., Balakrishnan, N., Vidakovic, B., and Johnson, N. L., doi:10.1002/0471667196.ess5050.pub2, 2006.

Nenes, A., Pandis, S. N., and Pilinis, C.: Continued development and testing of a new thermodynamic aerosol module for urban and regional air quality models, Atmos. Environ., 33, 1553–1560, doi:10.1016/S1352-2310(98)00352-5, 1999.

35 Neumann, D., Matthias, V., Bieser, J., Aulinger, A., and Quante, M.: A comparison of sea salt emission parameterizations in northwestern Europe using a chemistry transport model setup, Atmos. Chem. Phys., 16, 9905–9933, doi:10.5194/acp-16-9905-2016, 2016.

Neumann, D., Friedland, R., Karl, M., Radtke, H., Matthias, V., and Neumann, T.: Importance of high resolution nitrogen deposition data for biogeochemical modeling in the western Baltic Sea and the contribution of the shipping sector, Ocean Sci. Discuss., https://doi.org/10.5194/os-2018-71, in review, 2018a.

Neumann, D., Karl, M., Radtke, H., and Neumann, T.: Evaluation of atmospheric nitrogen inputs into marine ecosystems of the North Sea and Baltic Sea - part A: validation and time scales of nutrient accumulation, Biogeosciences Discuss., https://doi.org/10.5194/bg-2018-364, in review, 2018b.

Neumann, D., Radtke, H., Karl, M., and Neumann, T.: Evaluation of atmospheric nitrogen inputs into marine ecosystems of the North Sea and Baltic Sea - part B: contribution by shipping and agricultural emissions, Biogeosciences Discuss., https://doi.org/10.5194/bg-2018-365, in review, 2018c.

Odman, M. T., Hu, Y., Unal, A., Russell, A. G., and Boylan, J. W.: Determining the sources of regional haze in the southeastern U.S. using the CMAQ model, J. Appl. Meteorol. Climatol., 46(11), 1731–1743, doi:10.1175/2007JAMC1430.1, 2007.

Otte, T. L. and Pleim, J. E.: The Meteorology-Chemistry Interface Processor (MCIP) for the CMAQ modeling system: updates through MCIPv3.4.1, Geosci. Model Dev., 3, 243–256, doi:10.5194/gmd-3-243-2010, 2010.

Paerl, H. W.: Coastal Eutrophication in relation to atmospheric nitrogen deposition: Current perspectives, Ophelia, 41, 237–259, 1995.

Park, R. J., Jacob, D. J., Palmer, P. I., Clarke, A. D., Weber, R. J., Zondlo, M. A., Eisele, F. L., Bandy, A. R., Thornton, D. C., Sachse, G. W., and Bond, T. C.: Export efficiency of black carbon aerosol in continental outflow: Global implications, J. Geophys. Res., 110, D11205, doi:10.1029/2004JD005432, 2005.

Poupkou, A., Giannaros, T., Markakis, K., Kioutsioukis, I., Curci, G., Melas, D., and Zerefos, C.: A model for European Biogenic Volatile Organic Compound emissions: Software development and first validation, Environ. Modell. Softw., 25, 1845–1856, 2010.

Prank, M., Sofiev, M., Tsyro, S., Hendriks, C., Semeena, V., Francis, X. V., Butler, T., Denier van der Gon, H., Friedrich, R., Hendricks, H., Kong, X., Lawrence, M., Righi, M., Samaras, Z., Sausen, R., Kukkonen, J., and Sokhi, R.: Evaluation of the performance of four chemical transport models in predicting the aerosol chemical composition in Europe in 2005, Atmos. Chem. Phys., 16(10), https://doi.org/10.5194/acp-16-6041-2016, 2016.

Prank, M., Vira, J., Ots, R., and Sofiev, M.: Evaluation of Organic Aerosol and Its Precursors in the SILAM Model, In: Mensink C., Kallos G. (eds), Air Pollution Modeling and its Application XXV, ITM 2016, Springer Proceedings in Complexity, Springer, Cham, 2018.

Pye, H. O. T. and Pouliot, G. A.: Modeling the role of alkanes, polycyclic aromatic hydrocarbons, and their oligomers in secondary organic aerosol formation, Environ. Sci. Technol., 46, 6041–6047, doi:10.1021/es300409w, 2012.

Raudsepp, U., Laanemets, J., Maljutenko, I., Hongisto, M., and Jalkanen, J.-P.: Impact of ship-borne nitrogen deposition on the Gulf of Finland ecosystem: an evaluation, Oceanologia, 55(4), 837–857, doi:10.5697/oc.55-4.837, 2013.

Robinson, A. L., Donahue, N. M., Shrivastava, M. K., Weitkamp, E. A., Sage, A. M., Grieshop, A. P., Lane, T. E., Pierce, J. R., and Pandis, S. N.: Rethinking organic aerosols: semivolatile emissions and photochemical aging, Science, 315, 1259–1262, doi:10.1126/science.1133061, 2007.

Rockel, B., Will, A., and Hense, A.: The Regional Climate Model COSMO-CLM (CCLM), Meteorol. Z., 347–348, 2008.

Sarwar, G., Simon, H., Bhave, P., and Yarwood, G.: Examining the impact of heterogeneous nitryl chloride production on air quality across the United States. Atmos. Chem. Phys., 12, 6455–6473. doi:10.5194/acp-12-6455-2012, 2012.

Schaap, M., Cuvelier, C., Hendriks, C., Bessagnet, B., Baldasano, J. M., Colette, A., Thunis, P., Karam, D., Fagerli, H., Graff, A., Kranenburg, R., Nyíri, A., Pay, M. T., Rouïl, L., Schulz, M., Simpson, D., Stern, R., Terrenoire, E., and Wind, P.: Perfor-

mance of European chemistry transport models as function of horizontal resolution, Atmos. Environ., 112, 90-105, http://dx.doi.org/10.1016/j.atmosenv.2015.04.003 , 2015.

Schaub, D., Brunner, D., Boersma, K., Keller, J., Folini, D., Buchmann, B., Berresheim, H., and Staehelin, J.: SCIAMACHY tropospheric NO_2 over Switzerland: estimates of NO_X lifetimes and impact of the complex alpine topography on the retrieval, Atmos. Chem. Phys., 7, 5971–5987, doi:10.5194/acp-7-5971-2007, 2007.

Schwede, D., Pouliot, G., and Pierce, T.: Changes to the Biogenic Emissions Inventory System Version 3 (BEIS3), Proceedings of the 4th CMAS Models-3 Users' Conference 26–28 September 2005, Chapel Hill, NC, available at: http://www.cmascenter.org/conference/2005/abstracts/2_7.pdf, (Last Accessed 24.10.2018), 2005.

Shrivastava, M., Fast, J., Easter, R., Gustafson Jr., W. I., Zaveri, R. A., Jimenez, J. L., Saide, P., and Hodzic, A.: Modeling organic aerosols in a megacity: comparison of simple and complex representations of the volatility basis set approach, Atmos. Chem. Phys., 11, 6639–6662, 2011.

Simoens, D.: AirBase version 8 data products on EEA data service, European Environment Agency, available at: https://www.eea.europa.eu/data-and-maps/data/airbase-the-european-air-quality-database-8, (Last Accessed 24.10.2018), 2014.

Simpson, D.: Long-period modelling of photochemical oxidants in Europe. Model calculations for July 1985, Atmos. Environ., 26 A (9), 1609–1634, 1992.

Simpson, D., Butterbach-Bahl, K., Fagerli, H., Kesik, M., Skiba, U., and Tang, S.: Deposition and Emissions of Reactive Nitrogen over European Forests: A Modelling Study, Atmos. Environ., 40, 5712–5726, 2006a.

Simpson, D., Fagerli, H., Hellsten, S., Knulst, J. C., and Westling, O.: Comparison of modelled and monitored deposition fluxes of sulphur and nitrogen to ICP-forest sites in Europe, Biogeosciences, 3, 337–355, doi:10.5194/bg-3-337-2006, 2006b.

Simpson, D., Benedictow, A., Berge, H., Bergström, R., Emberson, L. D., Fagerli, H., Flechard, C. R., Hayman, G. D., Gauss, M., Jonson, J. E., Jenkin, M. E., Nyíri, A., Richter, C., Semeena, V. S., Tsyro, S., Tuovinen, J.-P., Valdebenito, Á., and Wind, P.: The EMEP MSC-W chemical transport model - technical description, Atmos. Chem. Phys., 12, 7825–7865, doi:10.5194/acp-12-7825-2012, 2012.

Simpson, D., Nyíri, A., Tsyro, S., Valdebenito, Á., and Wind, P.: Updates to the EMEP/MSC-W model, 2015-2016, In Transboundary particulate matter, photo-oxidants, acidifying and eutrophying components. EMEP Status Report 1/2016, 133–139, The Norwegian Meteorological Institute, Oslo, Norway, 2016.

Soares, J., Sofiev, M., Hakkarainen, J.: Uncertainties of wild-land fires emission in AQMEII phase 2 case study. Atmos. Environ., 115, 361–370, 2015.

Sofiev, M.: A model for the evaluation of long-term airborne pollution transport at regional and continental scales. Atmos. Environ. 34, 15, 2481–2493, 2000.

Sofiev, M., Genikhovich, E., Keronen, P., Vesala, T.: Diagnosing the surface layer parameters for dispersion models within the meteorological-to-dispersion modeling interface, J. of Appl. Meteorol. and Climatology, 49, 221–233, https://doi.org/10.1175/2009JAMC2210.1, 2010.

Sofiev, M., Soares, J., Prank, M., de Leeuw, G., Kukkonen, J.: A regional-to-global model of emission and transport of sea salt particles in the atmosphere, J. Geophys. Res. Atmos., 116, D21302, 4713, https://doi.org/10.1029/2010JD014713, 2011.

Sofiev, M., Vira, J., Kouznetsov, R., Prank, M., Soares, J., Genikhovich, E.: Construction of the SILAM Eulerian atmospheric dispersion model based on the advection algorithm of Michael Galperin, Geosci. Model Dev., 8, 3497–3522, https://doi.org/10.5194/gmd-8-3497-2015, 2015.

Sofiev, M., Kouznetsov, R., Prank, M., Soares, J., Vira, J., Tarvainen, V., and Sofieva, V.: A Long-Term Re-Analysis of Atmospheric Composition and Air Quality, in: Air Pollution Modeling and its Application XXV, edited by Mensink, C. and Kallos, G., pp. 55–59, Springer In-

ternational Publishing, Cham, https://link.springer.com/chapter/10.1007%2F978-3-319-57645-9_9, doi:10.1007/978-3-319-57645-9_9, 2018a.

Sofiev, M. Winebrake, J. J., Johansson, L., Carr, E. W., Prank, M., Soares, J., Vira, J., Kouznetsov, R., Jalkanen, J.-P., and Corbett, J. J.: Cleaner fuels for ships provide public health benefits with climate tradeoffs, Nature Communications, 9 (406), 1–12, doi:10.1038/s41467-017-02774-9, 2018b.

Solazzo, E., Bianconi, R., Pirovano, G., Matthias, V., Vautard, R., Moran, M. D., Appel, K. W., Bessagnet, B., Brandt, J., Christensen, J. H., Chemel, C., Coll, I., Ferreira, J., Forkel, R., Francis, X. V., Grell, G., Grossi, P., Hansen, A. B., Miranda, A. I., Nopmongcol, U., Prank, M., Sartelet, K. N., Schaap, M., Silver, J. D., Sokhi, R. S., Vira, J., Werhahn, J., Wolke, R., Yarwood, G., Zhang, J., Rao, S. T., and Galmarini, S.: Operational model evaluation for particulate matter in Europe and North America in the context of AQMEII, Atmos. Environ., 53, 75–92, doi:10.1016/j.atmosenv.2012.02.045, 2012a.

Solazzo, E., Bianconi, R., Vautard, R., Appel K. W., Moran, M. D., Hogrefe, C., Bessagnet, B., Brandt, J., Christensen, J. H., Chemel, C., Coll, I., Denier van der Gon, H., Ferreira, J., Forkel, R., Francis, X. V., Grell, G., Grossi, P., Hansen, A. B., Jeričević, A., Kraljević, L., Miranda, A. I., Nopmongcol, U., Pirovano, G., Prank, M., Riccio, A., Sartelet, K. N., Schaap, M., Silver, J. D., Sokhi, R. S., Vira, J., Werhahn, J., Wolke, R., Yarwood, G., Zhang, J., Rao, S. T., and Galmarini, S.: Model evaluation and ensemble modelling for surface-level ozone in Europe and North America in the context of AQMEII, Atmos. Environ., 53, 60–74, doi: 10.1016/j.atmosenv.2012.01.003, 2012b.

Solazzo, E., Bianconi, R., Pirovano, G., Moran, M. D., Vautard, R., Hogrefe, C., Appel, K. W., Matthias, V., Grossi, P., Bessagnet, B., Brandt, J., Chemel, C., Christensen, J. H., Forkel, R., Francis, X. V., Hansen, A. B., McKeen, S., Nopmongcol, U., Prank, M., Sartelet, K. N., Segers, A., Silver, J. D., Yarwood, G., Werhahn, J., Zhang, J., Rao, S. T., and Galmarini, S.: Evaluating the capability of regional-scale air quality models to capture the vertical distribution of pollutants, Geosci. Model Dev., 6, 791–818, https://doi.org/10.5194/gmd-6-791-2013, 2013.

Solazzo, E., Bianconi, R., Hogrefe, C., Curci, G., Tuccella, P., Alyuz, U., Balzarini, A., Baró, R., Bellasio, R., Bieser, J., Brandt, J., Christensen, J. H., Colette, A., Francis, X., Fraser, A., Vivanco, M. G., Jiménez-Guerrero, P., Im, U., Manders, A., Nopmongcol, U., Kitwiroon, N., Pirovano, G., Pozzoli, L., Prank, M., Sokhi, R. S., Unal, A., Yarwood, G., and Galmarini, S.: Evaluation and error apportionment of an ensemble of atmospheric chemistry transport modeling systems: multivariable temporal and spatial breakdown, Atmos. Chem. Phys., 17, 3001–3054, doi:10.5194/acp-17-3001-2017, 2017.

Song, C., Chen, G., Hanna, S., Crawford, J., and Davis, D.: Dispersion and chemical evolution of ship plumes in the marine boundary layer: Investigation of O_3/NO_y/HO_X chemistry, J. Geophys. Res., 108, doi:10.1029/2002JD002216, 2003.

Stjern, C. W., Samset, B. H., Myhre, G., Bian, H., Chin, M., Davila, Y., Dentener, F., Emmons, L., Flemming, J., Haslerud, A. S., Henze, D., Jonson, J. E., Kucsera, T., Lund, M. T., Schulz, M., Sudo, K., Takemura, T., and Tilmes, S.: Global and regional radiative forcing from 20 % reductions in BC, OC and SO_4 - an HTAP2 multi-model study, Atmos. Chem. Phys., 16(21), 13579–13599, doi:10.5194/acp-16-13579-2016, 2016.

Svensson, N., Bergström, H., Sahlée, E., and Rutgersson, A.: Stable atmospheric conditions over the Baltic Sea: model evaluation and climatology, Boreal Env. Res., 21, 387–404, ISSN: 1797-2469, 2016.

Textor, C., Schulz, M., Guibert, S., Kinne, S., Balkanski, Y., Bauer, S., Berntsen, T., Berglen, T., Boucher, O., Chin, M., Dentener, F., Diehl, T., Easter, R., Feichter, H., Fillmore, D., Ghan, S., Ginoux, P., Gong, S., Grini, A., Hendricks, J., Horowitz, L., Huang, P., Isaksen, I., Iversen, I., Kloster, S., Koch, D., Kirkevåg, A., Kristjansson, J. E., Krol, M., Lauer, A., Lamarque, J. F., Liu, X., Montanaro, V., Myhre, G., Penner, J., Pitari, G., Reddy, S., Seland, Ø., Stier, P., Takemura, T., and Tie, X.: Analysis and quantification of the diversities of aerosol life cycles within AeroCom, Atmos. Chem. Phys., 6, 1777–1813, doi:10.5194/acp-6-1777-2006, 2006.

Tsyro, S., Nyíri, A., and Wind, P.: Model calculations for 2013 in the new EMEP grid, In Transboundary particulate matter, photo-oxidants, acidifying and eutrophying components, EMEP/MSC-W Status Report 1/2015, The Norwegian Meteorological Institute, Oslo, Norway, 2015.

Tsyro, S., Aas, W., Solberg, S., Benedictow, A., Fagerli, H., and Posch, M.: Status of transboundary air pollution in 2016, In: Transboundary particulate matter, photo-oxidants, acidifying and eutrophying components, EMEP/MSC-W Status Report 1/2018, Norwegian Meteorological Institute (EMEP/MSC-W), Oslo, Norway, 204 pp., 2018.

van Aardenne, J., Colette, A., Degraeuwe, B., Hammingh, P., Viana, M., and Vlieger, I.: The impact of international shipping on European air quality and climate forcing, Technical Report No. 4/2013, EEA (European Environment Agency), Copenhagen, Denmark, 1–84, 2013.

Vautard, R., Moran, M. D., Solazzo, E., Gilliam, R. C., Matthias, V., Bianconi, R., Chemel, C., Ferreira, J., Geyer, B., Hansen, A. B., Jericevic, A., Prank, M., Segers, A., Silver, J. D., Werhahn, J., Wolke, R., Rao, S. T., and Galmarini, S.: Evaluation of the meteorological forcing used for the Air Quality Model Evaluation International Initiative (AQMEII) air quality simulations, Atmos. Environ., 53, 15–37, doi:10.1016/j.atmosenv.2011.10.065, 2012.

Viana, M., Hammingh, P., Colette, A., Querol, X., Degraeuwe, B., de Vlieger, I., and van Aardenne, J.: Impact of maritime transport emissions on coastal air quality in Europe, Atmos. Environ., 90, 96–105, http://dx.doi.org/10.1016/j.atmosenv.2014.03.046, 2014.

Vignati, E., Karl, M., Krol, M., Wilson, J., Stier, P., and Cavalli, F.: Sources of uncertainties in modelling black carbon at the global scale, Atmos. Chem. Phys., 10, 2595–2611, doi:10.5194/acp-10-2595-2010, 2010.

Vinken, G. C. M., Boersma, K. F., Jacob, D. J., and Meijer, E. W.: Accounting for non-linear chemistry of ship plumes in the GEOS-Chem global chemistry transport model, Atmos. Chem. Phys., 11, 11707–11722, doi:10.5194/acp-11-11707-2011, 2011.

Vivanco, M. G., Theobald, M. R., García-Gómez, H., Garrido, J. L., Prank, M., Aas, W., Adani, M., Alyuz, U., Andersson, C., Bellasio, R., Bessagnet, B., Bianconi, R., Bieser, J., Brandt, J., Briganti, G., Cappelletti, A., Curci, G., Christensen, J. H., Colette, A., Couvidat, F., Cuvelier, C., D'Isidoro, M., Flemming, J., Fraser, A., Geels, C., Hansen, K. M., Hogrefe, C., Im, U., Jorba, O., Kitwiroon, N., Manders, A., Mircea, M., Otero, N., Pay, M.-T., Pozzoli, L., Solazzo, E., Tsyro, S., Unal, A., Wind, P., and Galmarini, S.: Modeled deposition of nitrogen and sulfur in Europe estimated by 14 air quality model systems: evaluation, effects of changes in emissions and implications for habitat protection, Atmos. Chem. Phys., 18, 10199–10218, https://doi.org/10.5194/acp-18-10199-2018, 2018.

Von Glasow, R., Lawrence, M. G., Sander, R., and Crutzen, P. J.: Modeling the chemical effects of ship exhaust in the cloud-free marine boundary layer, Atmos. Chem. Physics, 3, 233–250, doi:10.5194/acp-3-233-2003, 2003

Vukovich, J. and Pierce, T.: The Implementation of BEIS3 within the SMOKE Modeling Framework, in: Proceedings of the 11th International Emissions Inventory Conference, Atlanta, Georgia, 15-18 April 2002, available online: http://www.epa.gov/ttn/chief/conference/ei11/modeling/vukovich.pdf, (Last Accessed 24.10.2018), 2002.

Wankmüller, R. and Mareckova, K.: Emissions for 2012, In: Transboundary particulate matter, photo-oxidants, acidifying and eutrophying components, EMEP Status Report 1/2014, Norwegian Meteorological Institute (EMEP/MSC-W), Oslo, Norway, 2014

Whitten, G. Z., Heo, G., Kimura, Y., McDonald-Buller, E., Allen, D. T., Carter, W. P. L., and Yarwood, G.: A new condensed toluene mechanism for Carbon Bond: CB05-TU, Atmos. Environ., 44 (40), 5346–5355, 2010.

WMO: WMO Statement on the status of the global climate in 2012, World Meteorological Organization (WMO), Report-No 1108, 33 pp., Geneva, Switzerland, available online: http://library.wmo.int/pmb_ged/wmo_1108_en.pdf, (Last Accessed 14.12.2018), 2013.

Yarwood, G., Rao, S., Yocke, M., and Whitten, G. Z.: Updates to the Carbon Bond Mechanism: CB05, Report to the U.S. Environmental Protection Agency, RT-04-00675, available online: http://www.camx.com/publications/default.aspx, (Last Accessed 24.10.2018), 2005.
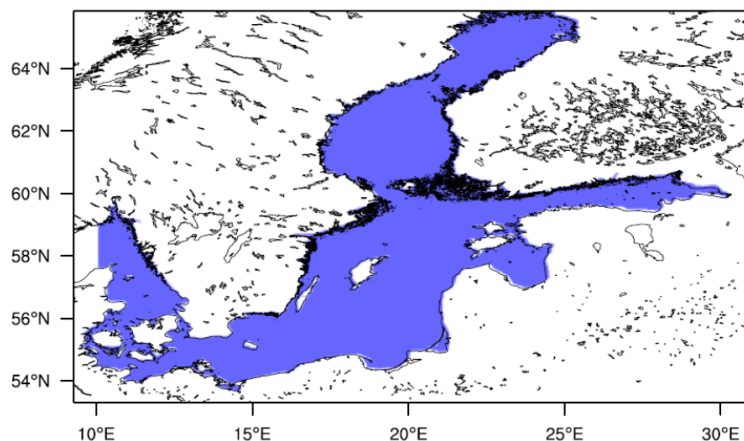
Figure 1. Geographic map of the study domain for the CTM comparison, spanning from latitude $53.40°N$ (south) to $65.80°N$ (north) and longitude $9.00°E$ (west) to $31.10°E$ (east). The extent of the Baltic Sea as used in this study is shown in blue.
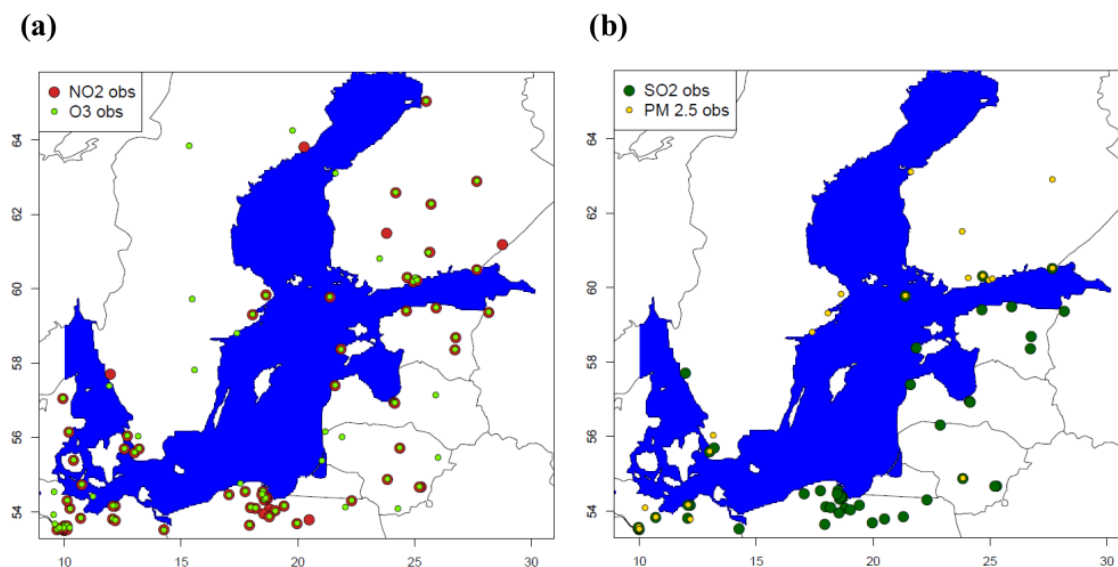
Figure 2. Map of the Baltic Sea region with the location of background monitoring stations used in the statistical performance analysis with observations of: (a) NO_2 (filled red circles) and O_3 (filled green circles); and (b) SO_2 (filled dark green circles) and $PM_{2.5}$ (filled yellow circles). Same domain extent as in Figure 1.

Atmospheric
Chemistry
and Physics
Discussions

(a)

(b)
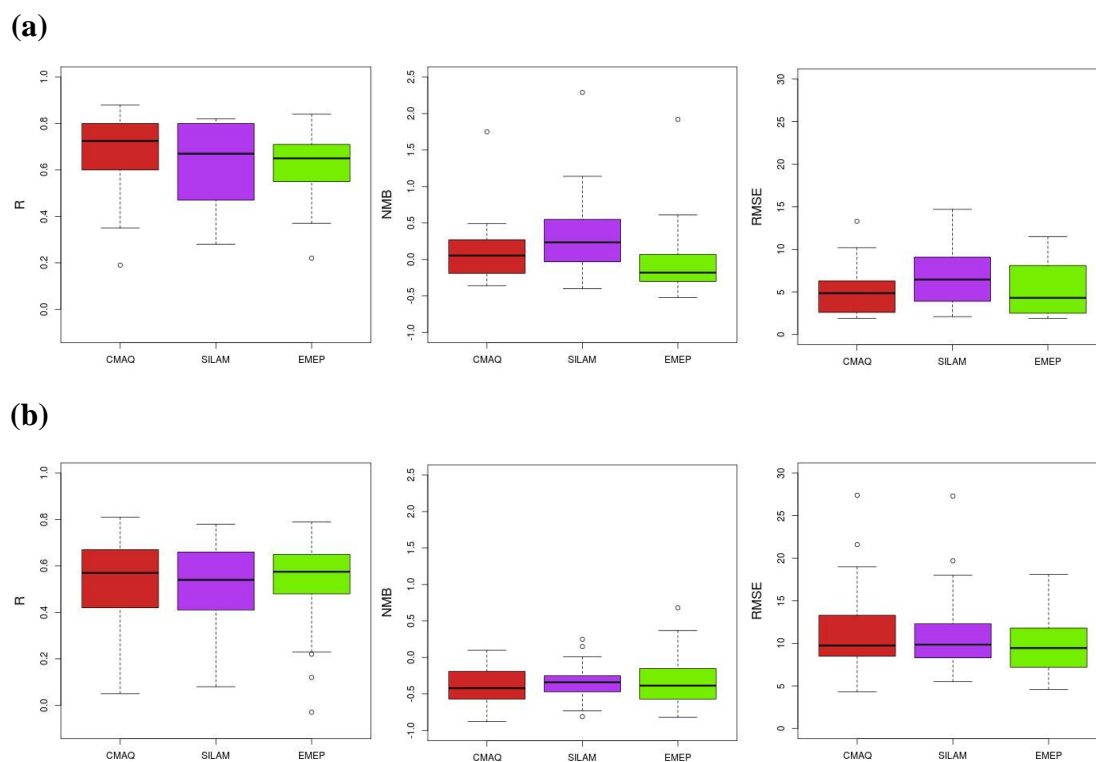
Figure 3. Comparison of statistical indicators for NO$_2$ daily means (in the order R, NMB, and RMSE) between three CTMs at: (a) rural background stations and (b) urban background stations. Outlier shown as small circles.

(a)

(b)
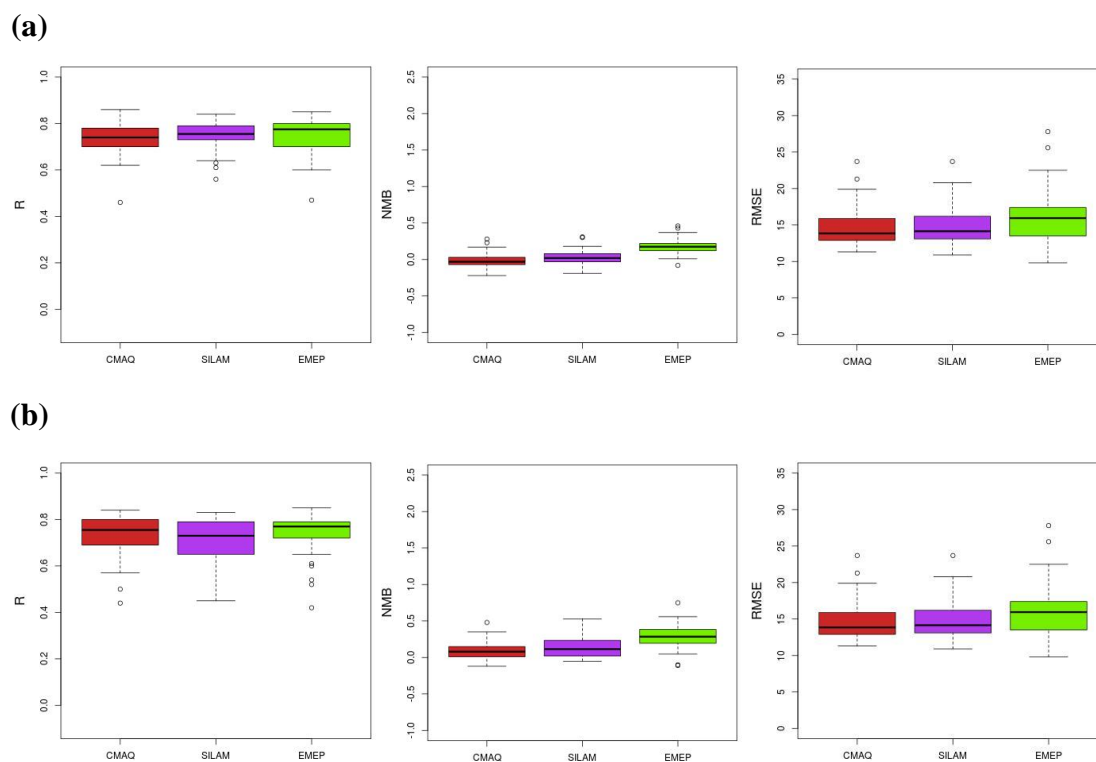
Figure 4. Comparison of statistical indicators for O$_3$ daily means (in the order R, NMB, and RMSE) between three CTMs at: (a) rural background stations and (b) urban background stations. Outlier shown as small circles.
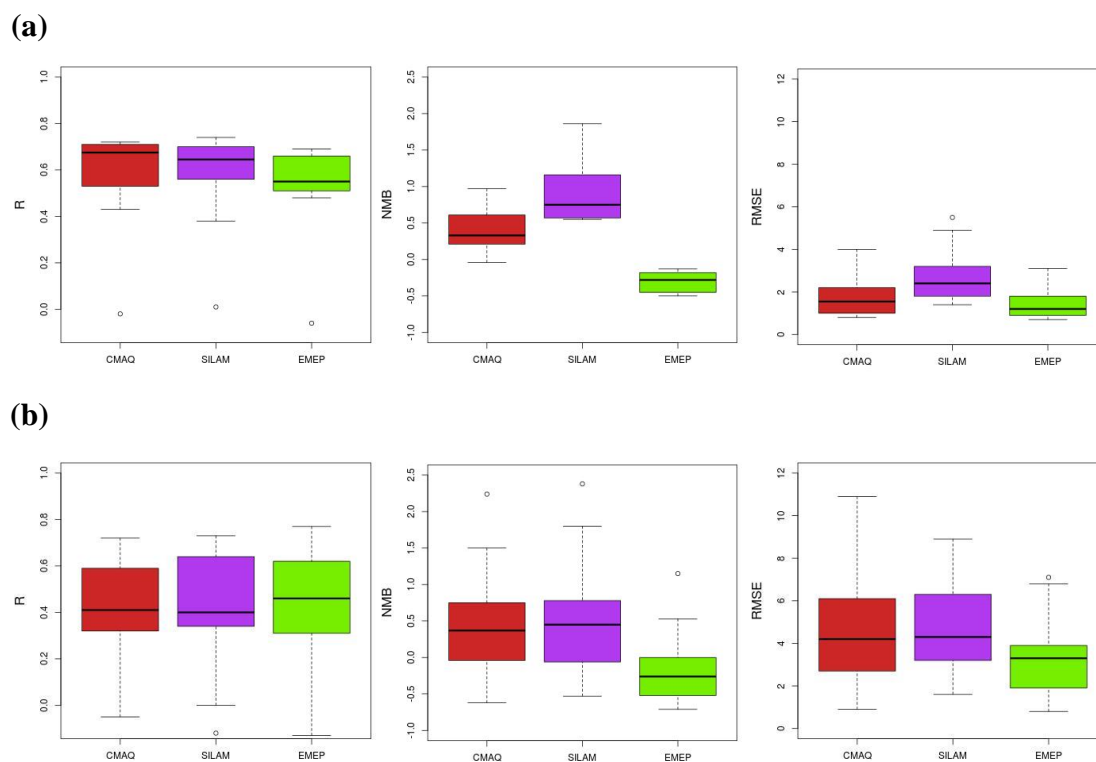
(a)

(b)

Figure 5. Comparison of statistical indicators for SO$_2$ daily means (in the order R, NMB, and RMSE) between three CTMs at: (a) rural background stations and (b) urban background stations. Outlier shown as small circles.

Figure 6. Comparison of statistical indicators for PM$_{2.5}$ daily means (in the order R, NMB, and RMSE) between three CTMs at: (a) rural background stations and (b) urban background stations. Outlier shown as small circles.
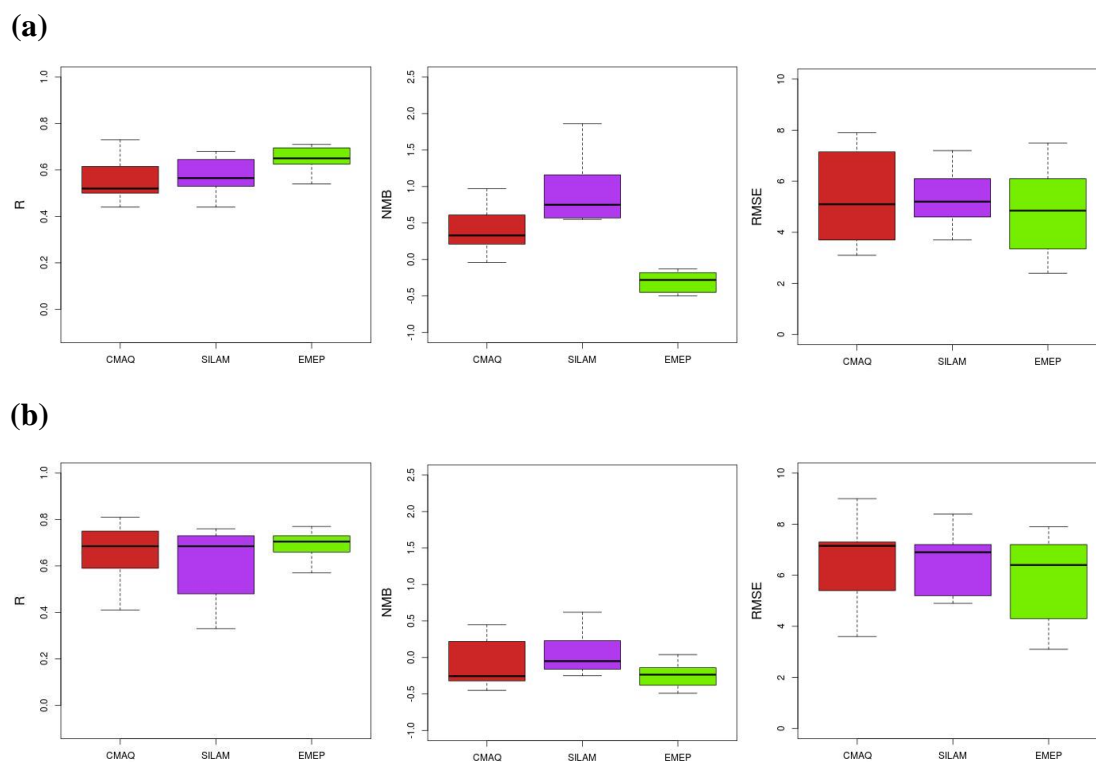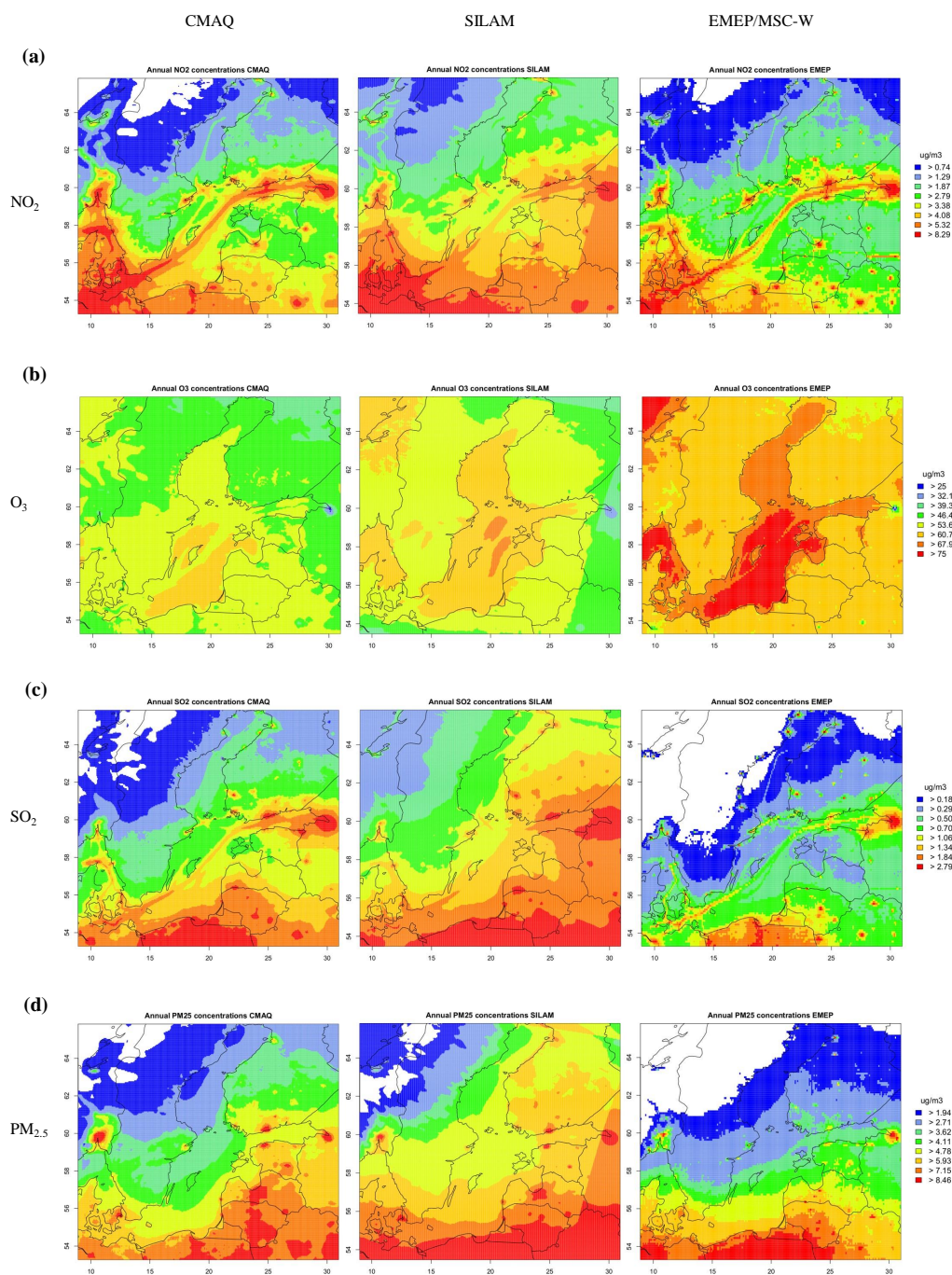
Figure 7. Comparison of the spatial distribution of annual mean concentrations ($\mu g\,m^{-3}$) from CMAQ (left column), SILAM (middle column) and EMEP (right column) in the Baltic Sea region for (a) O_3, (b) NO_2, (c) SO_2, and (d) $PM_{2.5}$. Empty areas correspond to concentrations between zero and the lowest value in the legend.

CMAQ   SILAM   EMEP/MSC-W

(a)

NO$_2$

(b)

O$_3$

(c)

SO$_2$

(d)

PM$_{2.5}$
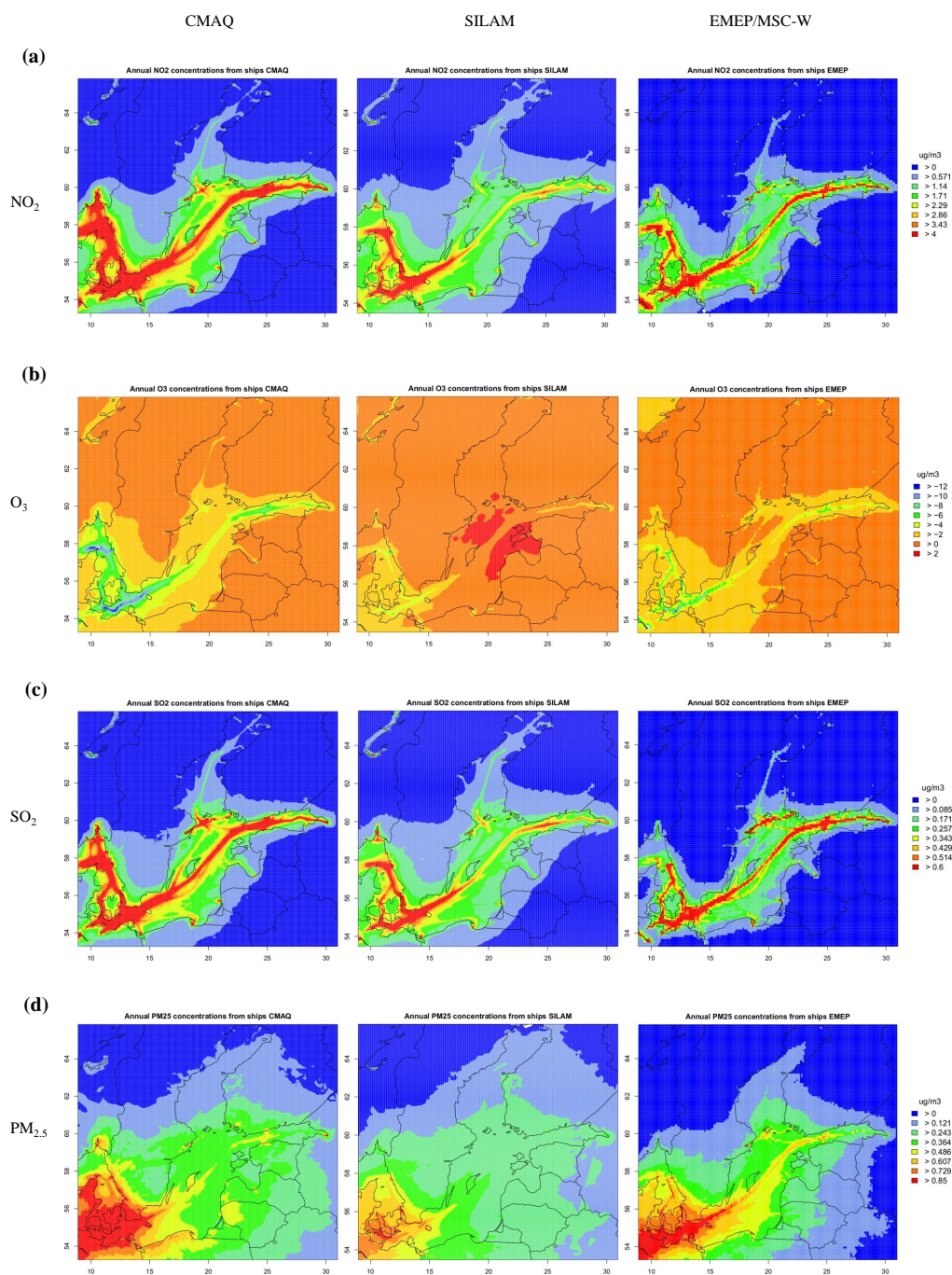
Figure 8. Comparison of the spatial distribution of annual mean ship-related concentrations (absolute ship contributions in μg m^{-3}) of the CMAQ (left column), SILAM (middle column) and EMEP (right column) models in the Baltic Sea region for (a) O$_3$, (b) NO$_2$, (c) SO$_2$, and (d) PM$_{2.5}$.
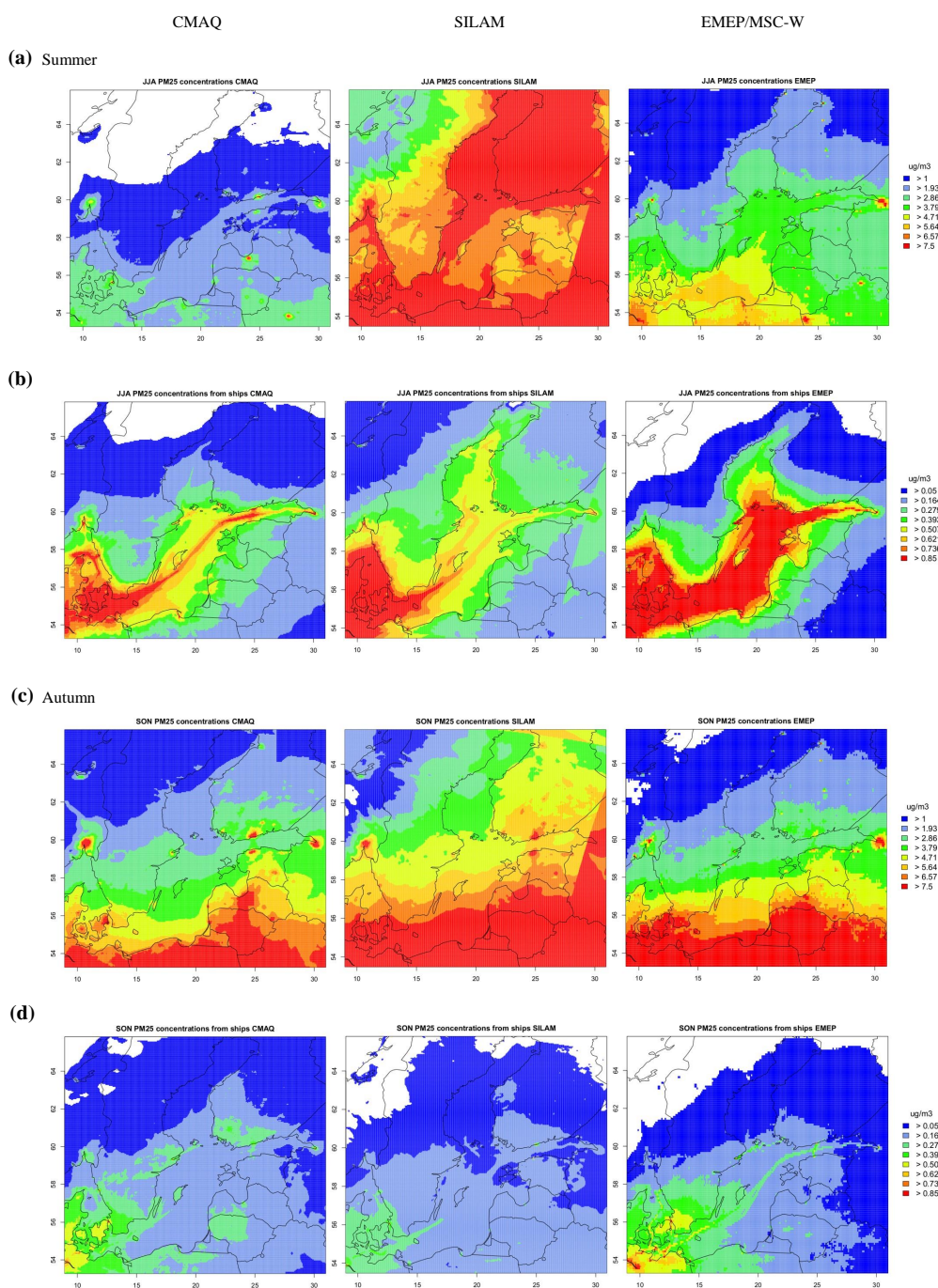
Figure 9. Comparison of PM$_{2.5}$ in summer and autumn from CMAQ (left column), SILAM (middle column) and EMEP (right column) in the Baltic Sea region for (a) JJA mean concentration (μg m^{-3}), (b) JJA mean ship contribution (μg m^{-3}), (c) SON mean concentration, and (d) SON mean ship contribution. Empty areas correspond to concentrations between zero and the lowest value in the legend.
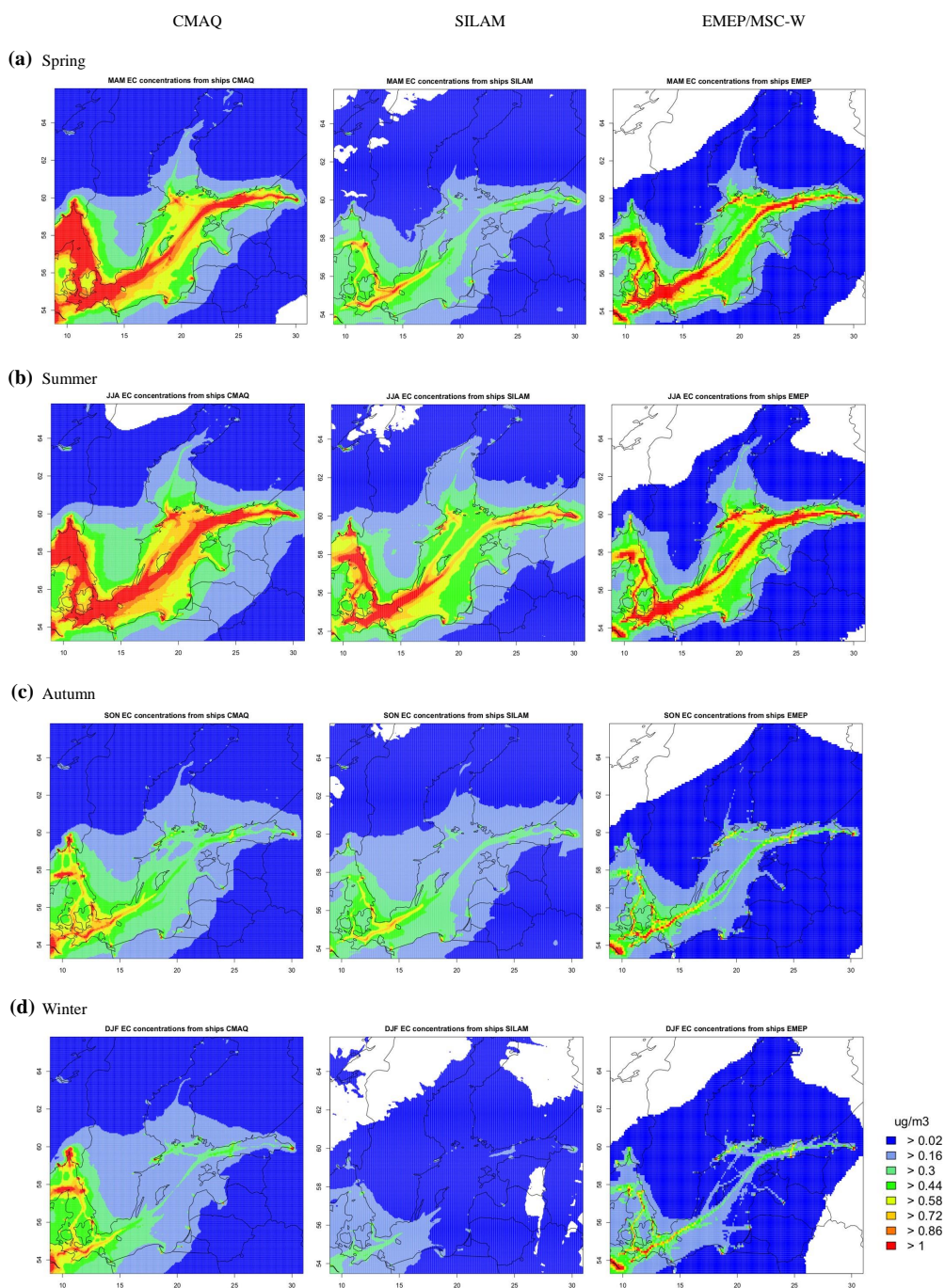
Figure 10. Spatial distribution of the seasonal mean EC ship contribution (μg m^{-3}) from CMAQ (left column), SILAM (middle column) and EMEP (right column) in the Baltic Sea region for (a) spring, (b) summer, (c) autumn, and (d) winter. Empty areas correspond to concentrations between zero and the lowest value in the legend.
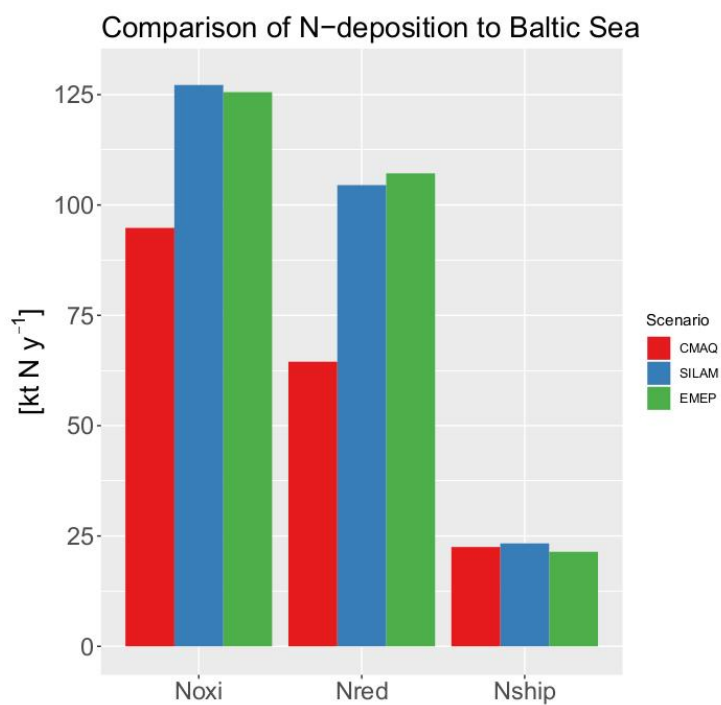
Figure 11. Comparison of the total annual deposition (ktN y^{-1}) of reduced and oxidised nitrogen and ship-related oxidised nitrogen (N$_{ship}$) to the Baltic Sea (seawater) from CMAQ (red), SILAM (dark blue) and EMEP/MSC-W (green).

Atmospheric
Chemistry
and Physics
Discussions

Table 1. Description of the model setup of the three CTM systems.

Model parameter	CMAQ	SILAM	EMEP/MSC-W
Horizontal grid resolution of the inner nest	$4 \times 4\,\mathrm{km}^2$	$4 \times 4\,\mathrm{km}^2$	$0.1° \times 0.1°$
Nesting	D1: 64 km D2: 16 km D3: 4 km	D1: ~70 km D2: ~18 km D3: 4 km	D1: 0.1°
Meteorological driver	COSMO-CLM	WRF	IFS-ECMWF, Cy40r1
Chemical boundary and initial conditions	FMI APTA global reanalysis	FMI APTA global reanalysis	Climatology for ozone
Land-based emissions	SMOKE-EU	SMOKE-EU	ECLIPSE
Ship emissions	STEAM $2 \times 2\,\mathrm{km}^2$	STEAM $2 \times 2\,\mathrm{km}^2$	STEAM $0.1° \times 0.1°$
Ship emission time variability	hourly	hourly	monthly

Table 2. Vertical profiles of ship emissions in the first seven vertical layers of the three CTM systems. The vertical distribution is given as average fractions of the total emission in each vertical model layer. Heights correspond to the heights of vertical layers in the models for a standard atmosphere.

Layer nr.	CMAQ		SILAM		EMEP/MSC-W	
	Height	Fraction	Height	Fraction	Height	Fraction
1	0–42 m	0.24	0–20 m	0.15	0–92 m	1.00
2	42–84 m	0.76	20–50 m	0.13	92–184 m	0
3	84–127 m	0	50–100 m	0.04	184–324 m	0
4	127–180 m	0	100–200 m	0.08	324–525 m	0
5	180–255 m	0	200–300 m	0.08	525–787 m	0
6	255–340 m	0	300–500 m	0.15	787–1116 m	0
7	340–430 m	0	500–1000 m	0.38	1116–1520 m	0

Atmospheric
Chemistry
and Physics
Discussions

Open Access

Table 3. Statistical evaluation of daily mean $PM_{2.5}$ for the year 2012 with all three CTMs.

Station code	N	μ_{Obs}	CMAQ					SILAM					EMEP/MSC-W				
			μ_{Mod}	R	NMB	RMSE	FAC2	μ_{Mod}	R	NMB	RMSE	FAC2	μ_{Mod}	R	NMB	RMSE	FAC2
DEHH008	363	12.6	9.8	0.73	-0.23	7.3	0.73	11.1	0.68	-0.12	7.2	0.86	10.8	0.71	-0.14	7.5	0.87
DEHH059	350	13.2	9.4	0.75	-0.28	7.3	0.65	11.1	0.76	-0.16	6.5	0.86	10.7	0.75	-0.18	7.1	0.87
DEMV019	364	12.9	7.1	0.79	-0.45	8.1	0.42	9.7	0.69	-0.25	7.9	0.77	8.0	0.73	-0.38	7.9	0.59
DEMV021	359	11.2	7.3	0.81	-0.35	6.5	0.55	8.8	0.75	-0.22	6.8	0.80	8.2	0.77	-0.27	6.4	0.73
DESH023	345	11.9	8.2	0.75	-0.31	7.2	0.63	10.0	0.73	-0.16	7.0	0.80	9.1	0.73	-0.23	7.2	0.76
FI00208	347	7.1	9.8	0.53	0.38	7.9	0.59	7.7	0.55	0.09	5.3	0.76	4.2	0.62	-0.41	4.9	0.56
FI00349	355	4.7	3.9	0.62	-0.17	3.1	0.58	5.3	0.55	0.12	4.7	0.61	3.4	0.63	-0.28	3.4	0.73
FI00351	364	7.4	5.2	0.44	-0.30	5.4	0.45	6.3	0.51	-0.14	5.6	0.67	3.4	0.63	-0.54	5.8	0.43
FI00586	357	5.9	4.0	0.64	-0.32	3.6	0.54	6.2	0.49	0.05	5.2	0.57	3.1	0.70	-0.49	4.3	0.55
FI00761	363	6.3	6.3	0.62	0.00	4.5	0.63	6.5	0.44	0.02	5.0	0.70	3.8	0.57	-0.39	4.3	0.63
FI00781	363	6.6	9.5	0.49	0.45	7.1	0.62	10.7	0.33	0.62	8.4	0.48	5.0	0.63	-0.24	4.0	0.82
LT00044	357	9.8	12.0	0.59	0.22	9.0	0.65	12.1	0.73	0.23	7.2	0.75	8.9	0.69	-0.09	6.4	0.78
SE0001A	338	11.0	6.4	0.61	-0.42	7.0	0.49	7.9	0.64	-0.28	6.6	0.67	6.9	0.71	-0.37	6.4	0.64
SE0011R	340	6.9	5.7	0.51	-0.17	4.8	0.57	7.0	0.65	0.01	5.1	0.75	5.8	0.68	-0.16	4.8	0.73
SE0012R	364	5.4	4.1	0.50	-0.24	3.8	0.52	5.4	0.58	-0.01	3.7	0.74	3.5	0.67	-0.36	3.3	0.64
SE0022A	358	4.8	6.7	0.41	0.39	5.4	0.67	6.9	0.48	0.42	4.9	0.66	5.0	0.66	0.04	3.1	0.86
SE0066A	345	3.3	4.1	0.50	0.25	3.6	0.58	5.3	0.44	0.60	4.5	0.47	3.2	0.54	-0.04	2.4	0.66

Table 4. Spatial averages of the annual mean concentrations of NO_2, O_3, SO_2, $PM_{2.5}$ and EC in $\mu g\,m^{-3}$ for the study domain (Baltic Sea region as in Fig. 1).

CTM	NO_2	O_3	SO_2	$PM_{2.5}$	EC
CMAQ	3.49	54.1	1.11	4.84	0.16
SILAM	4.42	57.6	1.61	5.95	0.15
EMEP/MSC-W	3.00	66.6	0.56	4.01	0.13

Atmospheric
Chemistry
and Physics
Discussions

Table 5. Relative ship contribution to the spatial average of annual mean NO_2, O_3, SO_2, $PM_{2.5}$ and EC in percent for the study domain (Baltic Sea region as in Fig. 1).

CTM	NO_2	O_3	SO_2	$PM_{2.5}$	EC
CMAQ	28.3	-0.4	14.5	6.5	7.3
SILAM	21.9	1.2	10.0	4.3	5.6
EMEP/MSC-W	21.8	-0.1	19.1	5.7	5.3

Table 6. Spatial averages of seasonal mean concentrations of EC ($\mu g\, m^{-3}$) from the "base" simulation and ship contributions to EC levels ($\mu g\, m^{-3}$) for the study domain (Baltic Sea region as in Fig. 1). Mean values are given for spring (March to May; MAM), summer (JJA), autumn (Sept. to Nov.; SON) and winter (January, February and December 2012; DJF)

Contribution	CTM	MAM	JJA	SON	DJF
	CMAQ	0.134	0.081	0.154	0.277
All emissions	SILAM	0.136	0.109	0.183	0.166
	EMEP/MSC-W	0.111	0.072	0.150	0.191
	CMAQ	0.013	0.014	0.009	0.008
Ship emissions	SILAM	0.007	0.011	0.007	0.003
	EMEP/MSC-W	0.008	0.009	0.005	0.004